iScience

CellPress
OPEN ACCESS

Article

Processing of matched and mismatched rNMPs in DNA by archaeal ribonucleotide excision repair

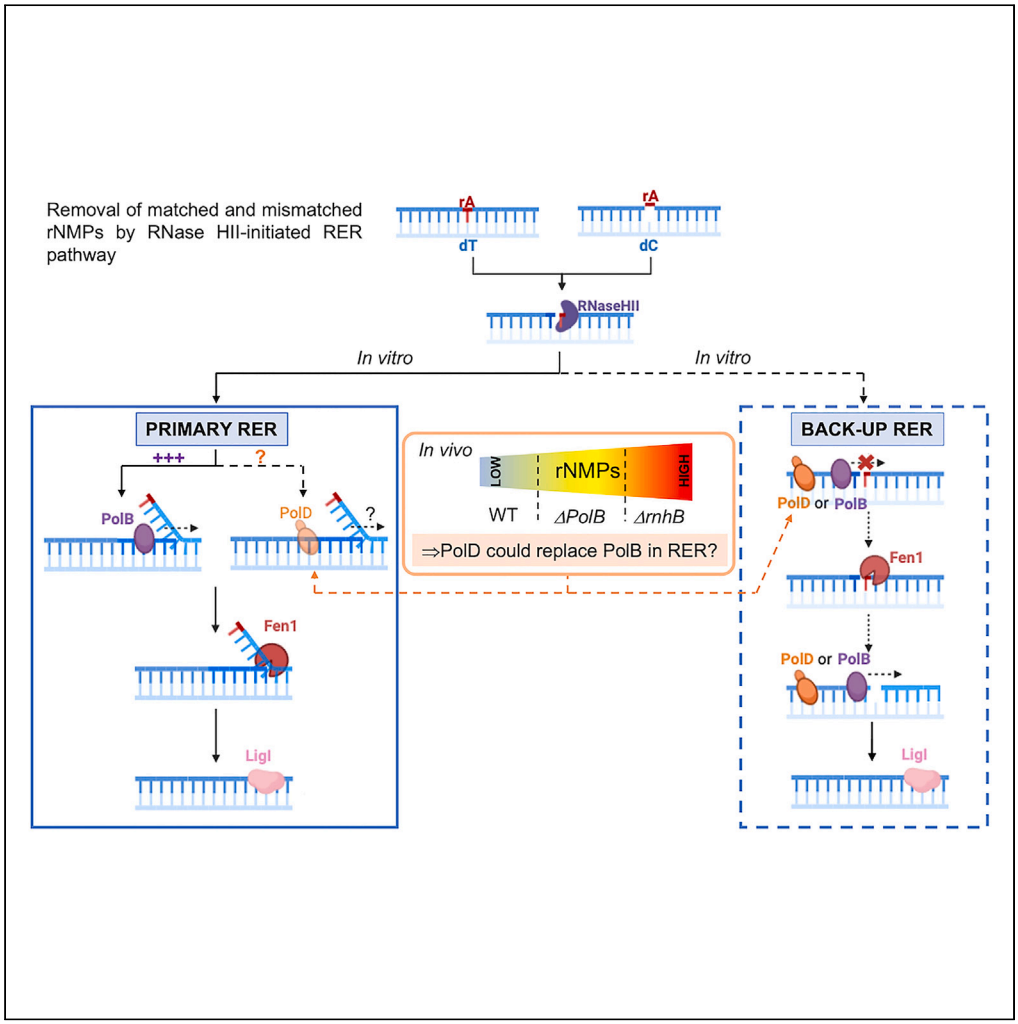

Maurane Reveil, Lucie Chapel, Blandine Vourc'h, ..., Yann Moalic, Mohamed Jebbar, Ghislaine Henneke

ghislaine.henneke@ifremer.fr

Highlights

RNase HII-mediated ribonucleotide excision repair can remove mispaired rNMPs in DNA

Identification of a backup RER mechanism on matched and mismatched rNMPs

The conserved RNase HII-initiated RER removes only parts of rNMPs in archaeal genome

In Archaea PolD can replace PolB in RNase HII-initiated RER with a lesser efficiency

Reveil et al., iScience 26, 108479
December 15, 2023
https://doi.org/10.1016/j.isci.2023.108479

iScience

CellPress
OPEN ACCESS

Article

Processing of matched and mismatched rNMPs in DNA by archaeal ribonucleotide excision repair

Maurane Reveil,[1] Lucie Chapel,[1] Blandine Vourc'h,[1] Audrey Bossé,[1] Léa Vialle,[1] Raphaël Brizard,[1] Yann Moalic,[1] Mohamed Jebbar,[1] and Ghislaine Henneke[1,2,*]

SUMMARY

Ribonucleoside monophosphates (rNMPs) are the main non-canonical nucleotides in genomic DNA, and their incorporation can occur as mismatches or matches *in vivo*. To counteract the mutagenic potential of rNMPs in DNA, all organisms evolved ribonucleotide excision repair (RER), a mechanism initiated by type 2 RNase H. Here, we describe the *in vitro* reconstitution of matched and mismatched rNMP repair using archaeal RER enzymes. Our data suggest two types of RER pathways, including the classical flap RER and a backup RER with the order of reactions changed for Fen1 and Pols. The genomic rNMP level in RER-deficient or PolB-deficient archaeal cells along with *in vitro* reconstitution of RER suggests an *in vivo* role of PolD in RER. Our results provide insights into how matched and mismatched rNMPs may be processed by RER.

INTRODUCTION

Ribonucleoside monophosphates (rNMPs) are the most frequent non-standard nucleotides occurring in the genome of all organisms. Embedded rNMPs in DNA arise *in vivo* due to (i) incorporation by DNA polymerases (Pol) because of the much higher intracellular rNTPs concentration compared to deoxyribonucleotide triphosphates (dNTPs),[1–4] (ii) a default in Okazaki fragment maturation,[5,6] or (iii) oxidation of the sugar moiety of DNA.[7] Transiently embedded rNMPs in DNA can act as positive signals for DNA transactions,[8,9] but their persistence leads to replication stress and genomic instabilities.[10–14] Accumulation of genomic rNMPs caused by defective ribonucleotide excision repair (RER) is associated with Aicardi-Goutières syndrome or systemic lupus erythematosus in human,[15,16] tumorigenesis in mice,[17–19] and mutagenesis in *Bacteria*.[4] To counteract their potentially detrimental effects, embedded rNMPs are primarily repaired by the type 2 Ribonuclease H (RNase HII/2) error-free RER mechanism which is conserved in all domains of life.[1,20,21] In the absence of functional RNase HII/2 in eukaryotes, a backup pathway involving DNA topoisomerase 1 may serve for the removal of rNMPs in DNA, although it is viewed as highly mutagenic processing.[22–26] In eukaryotes and *Bacteria*, other repair pathways ensure the removal of rNMPs in the genome like base excision repair (BER),[27] nucleotide excision repair (NER),[28] and mismatch repair (MMR).[29]

For now, RNase HII/2-initiated RER is the only evolutionary conserved pathway in all domains of life for rNMP removal.[1,20,21] The monomeric RNase HII in *Archaea* and *Bacteria* or the heterotrimeric RNase H2 in eukaryotes specifically incises the phosphodiester bond at the 5′-side of the embedded rNMP in DNA.[30,31] Archaeal RNase HII, the functional eukaryotic RNase H2 counterpart,[31] is not essential, and its knockout in Thermococcales does not affect cell growth[1,32,33] but induces an increase of genomic rNMPs incorporation.[1,2] In all organisms, RNase HII/2 cleavage at the RNA-DNA junctions leaves a 5′-phosphate ribonucleotide and a 3′-OH group, which is then extended by Pols. Through extension of the 3′-OH end, Polδ or Polε in eukaryotes or Pol I in *Bacteria* may perform strand displacement of the 5′-ribonucleotide-containing strand.[20,21,34] Although it is believed that PolB performs strand-displacement synthesis of the 5′-rNMP strand in *Archaea*,[1] a PolD-mediated RER cannot be excluded. In *Bacteria*, the resulting displaced rNMP-containing strand is then degraded by the 5′-3′ exonuclease or 5′-flap endonuclease activity of Pol I before DNA ligase (Lig) ends the repair.[21,34] In eukaryotes and *Archaea*, the displaced 5′-rNMP strand is cut by flap endonuclease Fen1 (or the exonuclease Exo1 in yeast) before ligation by Lig1.[1,20]

Despite recent *in vitro* and *in vivo* evidences of RNase HII/2 incision at single mispaired rNMPs,[29,35] *in vitro* reconstitution of RER mechanisms are only relevant for matched rNMP-containing substrates.[1,20,21] This is likely because there is no report about genomic detection of mismatched ribonucleotides. Nonetheless, several studies support the formation of mispaired rNMPs in DNA in different species. One of ours showed that rA is the most incorporated rNMP in DNA as a match (~95%) or a mismatch (~13%) by archaeal PolD and that dA is the most incorporated dNMP as a mismatch (~16%) opposite template rC base.[2] Other results showed that mispaired rNMPs occur during translesion

[1]University Brest, CNRS, Ifremer, UMR6197 Biologie et Ecologie des Ecosystèmes marins Profonds, 1625 Rte de Sainte-Anne, 29280 Plouzané, France
[2]Lead contact
*Correspondence: ghislaine.henneke@ifremer.fr
https://doi.org/10.1016/j.isci.2023.108479

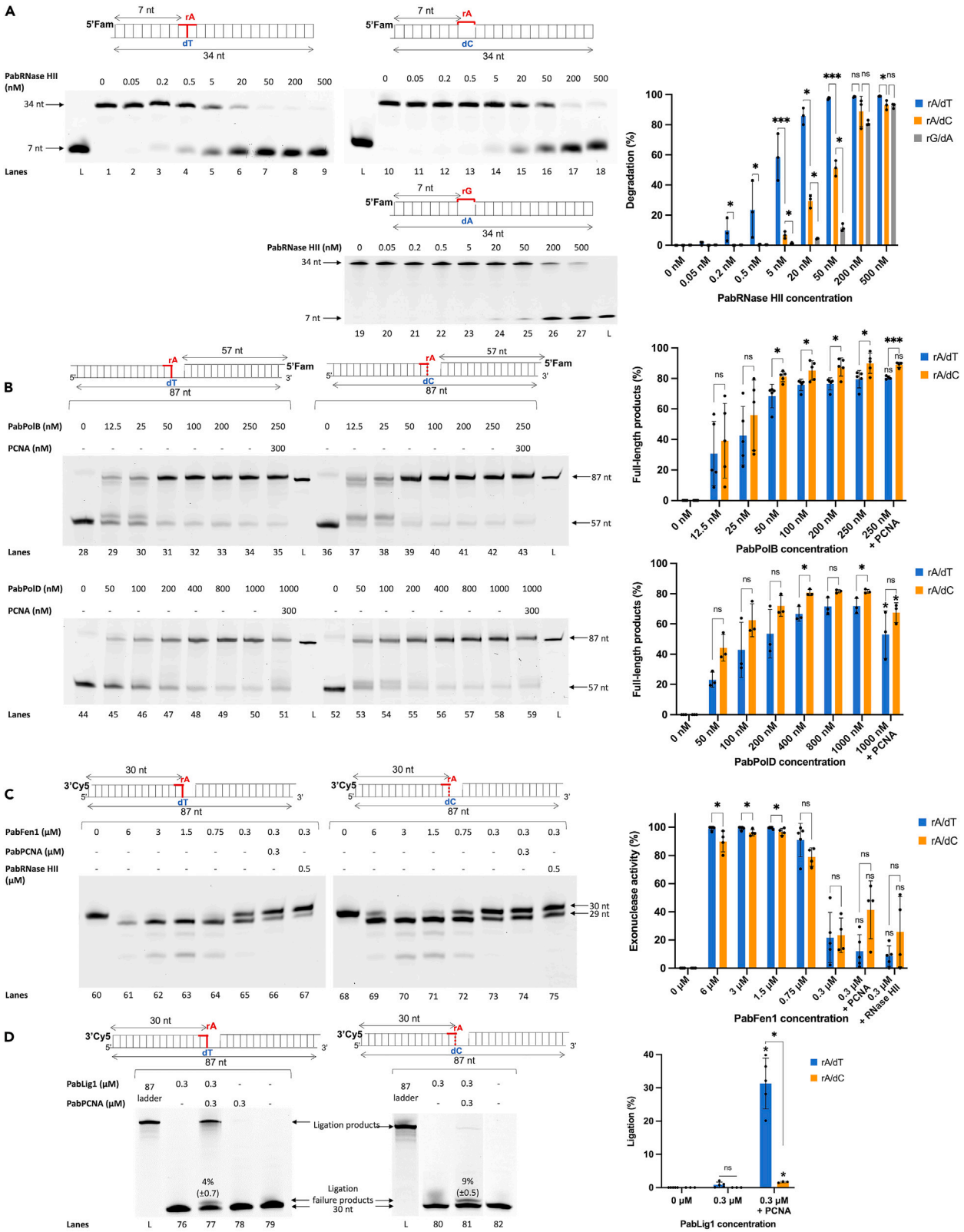
A
7 nt
rA
5'Fam
dT
34 nt
dC
PabRNase HII (nM)
0 0.05 0.2 0.5 5 20 50 200 500
34 nt
7 nt
Lanes
L 1 2 3 4 5 6 7 8 9
L 10 11 12 13 14 15 16 17 18
rG
dA
19 20 21 22 23 24 25 26 27 L
Degradation (%)
rA/dT
rA/dC
rG/dA
0 nM 0.05 nM 0.2 nM 0.5 nM 5 nM 20 nM 50 nM 200 nM 500 nM
PabRNase HII concentration
B
57 nt
87 nt
PabPolB (nM)
0 12.5 25 50 100 200 250 250
PCNA (nM)
300
87 nt
57 nt
28 29 30 31 32 33 34 35 L 36 37 38 39 40 41 42 43 L
Full-length products (%)
0 nM 12.5 nM 25 nM 50 nM 100 nM 200 nM 250 nM 250 nM + PCNA
PabPolB concentration
PabPolD (nM)
0 50 100 200 400 800 1000 1000
44 45 46 47 48 49 50 51 L 52 53 54 55 56 57 58 59 L
0 nM 50 nM 100 nM 200 nM 400 nM 800 nM 1000 nM 1000 nM + PCNA
PabPolD concentration
C
30 nt
29 nt
3'Cy5
PabFen1 (μM)
0 6 3 1.5 0.75 0.3 0.3 0.3
PabPCNA (μM)
PabRNase HII (μM)
0.5
60 61 62 63 64 65 66 67 68 69 70 71 72 73 74 75
Exonuclease activity (%)
0 μM 6 μM 3 μM 1.5 μM 0.75 μM 0.3 μM 0.3 μM + PCNA 0.3 μM + RNase HII
PabFen1 concentration
D
PabLig1 (μM)
87 ladder
Ligation products
4% (±0.7)
Ligation failure products 30 nt
9% (±0.5)
76 77 78 79 L 80 81 82
Ligation (%)
0 μM 0.3 μM 0.3 μM + PCNA
PabLig1 concentration

Figure 1. Enzymatic characterization of RER enzymes on matched or mismatched substrates

Lanes L contain oligonucleotide ladders. The structure of matched or mismatched dsDNA substrates are shown at the top of each gel, and oligonucleotide sequences are in Table S3. Bar graphs are the means ± standard deviation of cleavage products of at least three independent experiments. p values were determined by unpaired t test and are reported: ***p value <0.0001, *p value <0.05 and non-significant (ns). The p values represented above the bars when PabPCNA or PabRNaseHII are added to the reactions correspond to the difference observed with the condition of the same enzyme concentration without PabPCNA or PabRNase HII.

(A) Ribonuclease activity of PabRNase HII. The indicated amounts of PabRNase HII were incubated with matched L34_rA/L34_dT (lanes 1–9), mismatched L34_rA/L34_dC (lanes 10–18), or L34_rG/L34_dA_reverse (lanes 19–27).

(B) Strand-displacement activity of PabPolB and PabPolD. The indicated amounts of PabPolB or PabPolD were incubated with matched L30_rA:L57RC/L87 (lanes 29–34 and 45–50, respectively), mismatched L30_rA:L57RC/L87_dC (lanes 37–42, 53–58, respectively) or with PabPCNA (lanes 35, 51, 43, 59).

(C) 5′-3′ exonuclease and 5′-flap endonuclease activities of PabFen1. The indicated amounts of PabFen1 were incubated with matched L30_rA:L57RC/L87 (lanes 60–67) or mismatched L30_rA:L57RC/L87_dC (lanes 68–75) without PabPCNA or with 0.3 μM PabPCNA (lanes 66, 74) or 0.5 μM PabRNase HII (lanes 67, 75).

(D) Ligation activity of PabLig1. The indicated amounts of PabLig1 were incubated with matched L30_rA:L57RC/L87 in the absence or presence of 0.3 μM PabPCNA (lanes 76–77, respectively) or with mismatched rA/dC L30_rA:L57RC/L87_dC in the absence or presence of 0.3 μM PabPCNA (lanes 80–81, respectively) and 1 mM ATP.

synthesis of 7,8-dihydro-8-oxoguanine by bacterial DinB2 Pol.[36] In eukaryotes, findings revealed the formation of mismatch-containing ribonucleotides and oxidized template bases by Polβ[37] as well as stable formation of oxidized rGMP (guanosine monophosphate) by Polμ.[38] Therefore, in this study we ask whether the conserved RER pathway, known to operate on matched rNMPs, can also be involved in the removal of mismatched rNMPs. Using *Archaeal* RER enzymes, RNase HII, DNA Pols (PolD and PolB), Lig1, and Fen1 in test substrate *in vitro*, we show that mispaired rNMPs can be repaired by the conserved RER. We also identify a backup RNase HII/2-mediated RER mechanism on both matched and mismatched rNMPs in which the order of action is changed for Fen1 and DNA Pol. Finally, our *in vivo* analysis corroborates *in vitro* results, showing that the RER pathway removes genomic rNMPs with RNase HII being the key enzyme.

RESULTS

PabRNase HII can specifically cleave a mismatched rAMP with lesser efficiency than a matched rAMP

Our previous study showed that rAMP (adenosine monophosphate) was the most incorporated rNMP as a match or a mismatch by PabPolD.[2] We thus first compared the cleavage activities of PabRNase HII on substrates containing a matched or mismatched rAMP embedded in a 34-nt dsDNA (double-stranded DNA) sequence (Figure 1A). When the matched rA/dT was incubated with increasing amounts of PabRNase HII, a major 7-nt product appeared (Figure 1A lanes 3–9) and complete hydrolysis was observed at 50 nM (Figure 1A lane 7, blue bars). These results indicate that PabRNase HII specifically cleaves at the 5′-side of the matched rAMP-containing DNA substrate. PabRNase HII was also effective on a mismatched rA/dC, generating 7-nt products (Figure 1A lanes 14–18), but full degradation required at least 500 nM (Figure 1A lane 18, orange bars). PabRNase HII is thus more efficient to cleave a matched rAMP compared to a mismatched rAMP-containing DNA substrate (Figure 1A, blue and orange bars). However, this result seems to differ from a previous study showing the undetectable activity of PabRNase HII or human RNase H2 on mismatched rGMP-containing DNA substrate.[31] For clarification, we thus assessed PabRNase HII activity in our experimental conditions on the same substrate as in Malfatti et al.,[31] an rGMP embedded in a 34-nt dsDNA opposite dAMP (deoxyadenosine monophosphate)(Figure 1A lanes 19–27). The mismatched rG/dA was cleaved by PabRNase HII at concentrations starting from 20 nM (Figure 1A lanes 24–27, gray bars) but less efficiently than matched rA/dT and mismatched rA/dC (Figure 1 orange and blue bars compared with gray bars). Complete hydrolysis was never obtained for the rG/dA mismatch (Figure 1A, gray bars). These results indicate that in our experimental conditions, PabRNase HII is less effective on a mismatched rG/dA compared to a mismatched rA/dC suggesting that PabRNase HII activity seems to be influenced by the identity of the mismatched base pair. Overall, these data demonstrate that PabRNase HII maintains its ability to process not only a matched rNMP embedded in DNA but also a mismatched rNMP with lesser efficiency, leaving a monoribonucleotide attached to the DNA strand.

PabPolB and PabPolD strand-displacement activities are efficient on a matched or mismatched 5′-rAMP-containing DNA template

PabPolB and PabPolD strand-displacement activity was then assessed individually on 5′-matched or mismatched rAMP nicked templates, corresponding to the intermediate generated by PabRNase HII incision in RER (Figure 1B). To obtain at least 70% of full-length products (87-nt) by extension of the 57-nt primer and displacement of the matched or mismatched 5′-rAMP downstream strand, 50 nM of PabPolB were necessary (Figure 1B lanes 31, 39, bar graphs), whereas 800 nM and 200 nM of PabPolD were required, respectively (Figure 1B lanes 49, 55, bar graphs). The maximal strand-displacement activity on both mismatched rA/dC or matched rA/dT dsDNA templates was reached at 250 nM of PabPolB and 1,000 nM of PabPolD (Figure 1B lanes 34, 42 for PolB and 50, 58 for PolD, bar graphs). At these concentrations, PabPolB and PabPolD displaced more efficiently the downstream strand containing 5′-rAMP mismatches than the matches (Figure 1B lanes 34, 42 for PabPolB, 50, 58 for PabPolD, orange and blue bar graphs). This displacement was not significantly affected by PabPCNA (proliferating cell nuclear antigen), albeit slightly increasing a small fraction of unused and shorter extension primers by PabPolD (Figure 1B

lanes 34, 42, 50, 58 compared to 35, 43, 51, 59, respectively, bar graphs). Taken together, these results show that PabPolD strand-displacement activity of a matched or mismatched 5′-rAMP downstream strand is less efficient than PabPolB.

PabFen1 5′-3′ exonuclease and 5′-flap endonuclease activities are able to remove 5′-matched and mismatched rNMP-containing substrates after PabRNase HII incision

In RER, Fen1 endonuclease activity has been largely studied in cleaving flap structures.[1,20,39] In contrast, there is little concern about rNMP removal by Fen1 5′-3′ exonuclease activity, while this is reminiscent of RNA primer removal in Okazaki fragment processing.[40–42] Thus, we assessed 5′-flap endonuclease and 5′-3′ exonuclease activities of PabFen1 on different substrates that mimic relevant RER intermediates. First, PabFen1 endonuclease activity was measured on single- and double-flap substrates[43,44] (Figure S1A). On single 16-nt 5′-flap substrate, 16-nt products were mainly generated and shorter fragments (14-15-nt) were faintly detectable (Figure S1A lanes 2–6). These results indicate that PabFen1 endonuclease is active on single 5′-flap substrates, cutting at the flap junction in dsDNA and less frequently 1 or 2-nt before the junction in the flap structure. On the double-flap substrate containing a 1-nt 3′-tail, known as a cellular substrate,[43] PabFen1 endonucleolytic cleavage gave exclusively 17-nt products (Figure S1A lanes 10–16), corresponding to the precise cutting at a single position one nucleotide into the annealed region. As previously observed for eukaryotic Fen1,[43,45,46] PabFen1 endonuclease activity is more specific on double-flap than single-flap structures (Figure S1A lanes 10–16 compared to lanes 2–8).

Because 5′-rNMP nicked or nicked-flap templates reflect structural intermediates generated by RNase HII cleavage in RER, we analyzed if these substrates were stimulatory to PabFen1 5′-3′ exonuclease and 5′-flap endonuclease activities. Two dsDNA substrates were designed with the downstream strand annealed to the DNA template containing a 5′-phosphorylated rAMP matched (rA/dT) or mismatched (rA/dC) and dAMP matched (dA/dT) or mismatched (dA/dC) as depicted in Figures 1C and S1B, respectively. Phosphorylation of the 5′-rNMP nicked rA/dT template was a prerequisite in order to detect 5′-3′ exonuclease activity as previously published.[47] PabFen1 exonuclease and endonuclease activities were detectable on both 5′-rAMP matched (Figure 1C lanes 61–67) and mismatched substrates (Figure 1C lanes 69–75), releasing major 29-nt products. In this case, hydrolysis occurs one nucleotide into the labeled downstream strand and cleavage efficiencies were similar among matched and mismatched 5′-rAMP (Figure 1C, blue and orange bars, respectively). Additional fragments, shorter than the major products, were also found (Figure 1C lanes 61–64, 69–72). As for 5′-rAMP substrates, PabFen1 displays exonuclease and endonuclease activities on 5′-dAMP matched (Figure S1B lanes 18–24) and mismatched (Figure S1B lanes 26–32) substrates. The same cleavage patterns consisting of major 29-nt products and minor fragments were obtained (Figure S1B lanes 18–21, 26–29). Unexpectedly, PabFen1 exonuclease and endonuclease activities were slightly more efficient on matched or mismatched 5′-rAMP substrates (Figure 1C blue and orange bars, respectively) than on a matched or mismatched 5′-dAMP substrates (Figure S1B light blue and light orange bars, respectively) with or without PabPCNA or PabRNase HII (Figure 1C lanes 65–67, 73–75 and S1B lanes 22–24, 30–32). Overall, these results show that PabFen1 5′-3′ exonuclease and 5′-flap endonuclease activities are able to remove 5′-matched and mismatched rNMP-containing substrates which are relevant of PabRNase HII incision.

PabLig1 is able to ligate a 5′-rNMP nicked substrate only in the presence of PabPCNA

Because the reaction intermediate obtained after RNase HII incision is a nicked template representing a potentially ligatable substrate, we sought to assess whether PabLig1 was active on it. Ligation substrates were the same as for PabFen1 cleavage activities and are represented in Figures 1D and S1C. As expected, PabLig1 was active on the nicked substrate containing matched dNMP ends (42%), and its end-joining ability was not significantly affected by PabPCNA (Figure S1C lanes 1–2, light blue bars). Ligation was barely detectable on the nicked substrate with the 5′-dAMP mismatch, and a very faint 31-nt band appears (Figure S1C lane 5, light orange bars). This result shows that ligation reaction is not favorable in the presence of a mismatched 5′-DNA end, which is accompanied by accumulation of abortive 5′-AMP products (Figure S1C lane 5). These ligation failure products have already been observed with functional equivalents in *Bacteria* and eukaryotes, which were indicative of poor substrates for DNA ligases.[48–51] When ligation was examined on matched or mismatched 5′-rAMP nicked template, no activity was clearly measurable (Figure 1D lanes 76, 80, respectively). Interestingly, when PabPCNA was supplied to the reaction, ligation products (87-nt) corresponding to the nick sealing of a mismatched 5′-dAMP or matched 5′-rAMP were detectable (30%) as well as low amounts of 5′-AMP intermediates (4%) (Figure S1C lane 6, light orange bars and 1D lane 77, blue bars). In the presence of the rA/dC mismatch and PabPCNA, ligation was very weak, and higher amounts of ligation failure products (9%) were observed (Figure 1D lane 81, orange bars). Collectively, these results show that PabPCNA enhances PabLig1 activity on rA/dT matched, rA/dC and dA/dC mismatched nicked substrates. However, rA/dC mismatched templates remain poor substrates.

Both PabPolB and PabPolD can act in RNase HII-initiated RER pathway

The data presented in Figure 1 provided insights on the action of individual enzymes (RNase HII, Fen1, Lig1, Pols) when titrated on proper substrate, allowing fine-tuning of the enzyme ratios required for optimal RER reconstitution assay. Experimental conditions are the same as those for individual enzymes (Figures 1 and S1) and utilize our reaction buffer previously determined with the same enzymes.[52] RER reactions contain physiological concentrations of dNTPs as published before,[2] and double-labeled dsDNA templates with either a matched rA/dT (Figures 2A–2C) or a mismatched rA/dC (Figures 2D–2F) base pair. Double labeling of the top strand allows the simultaneous detection of resulting products in a single reaction, which are depicted in each figure panels (Figures 2, S2, and S3) and further described in STAR methods.

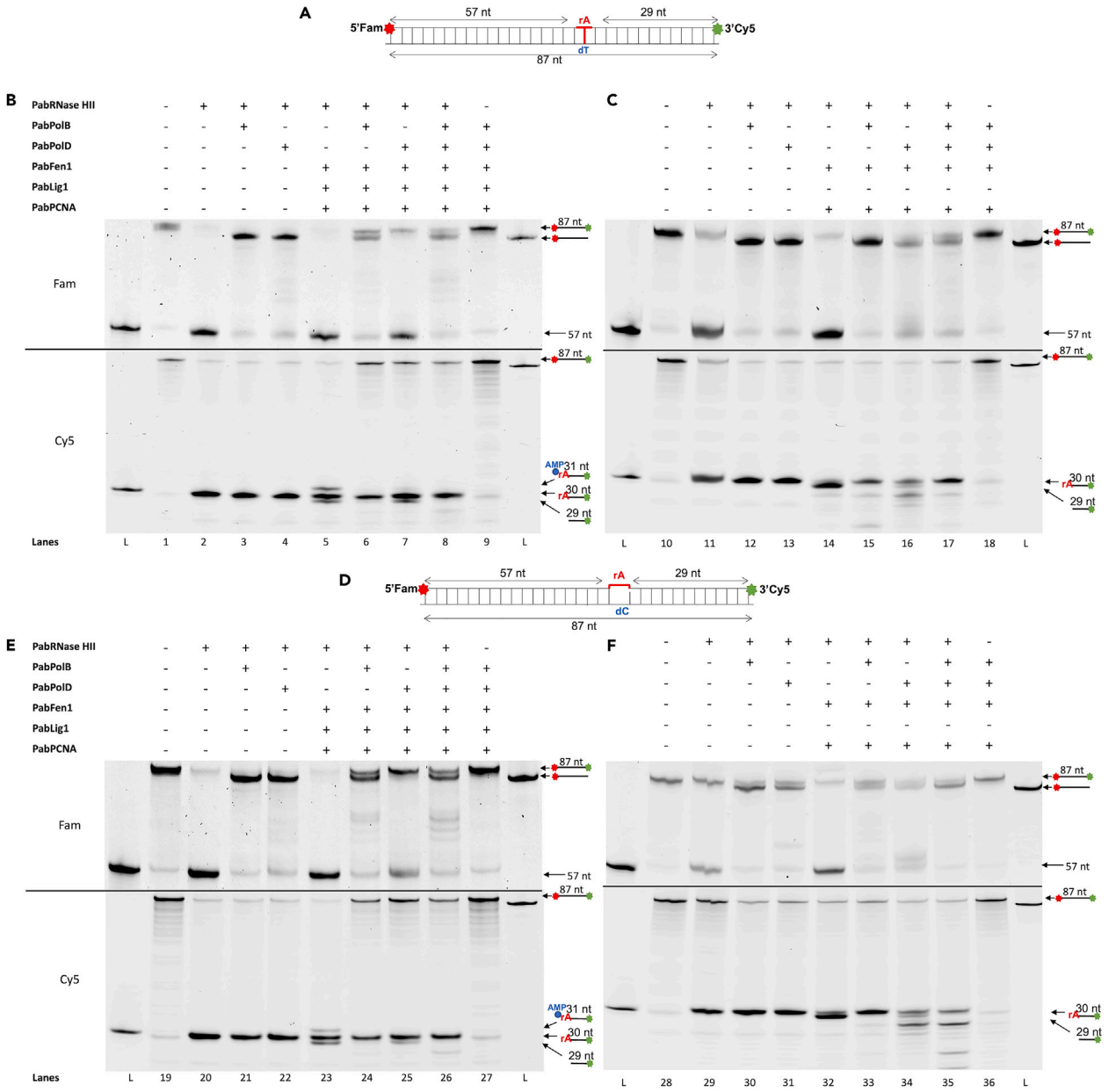
A
5'Fam
57 nt
rA
29 nt
3'Cy5
dT
87 nt
B
PabRNase HII
PabPolB
PabPolD
PabFen1
PabLig1
PabPCNA
Fam
Cy5
87 nt
57 nt
AMP
31 nt
30 nt
29 nt
Lanes
L 1 2 3 4 5 6 7 8 9 L
C
L 10 11 12 13 14 15 16 17 18 L
D
5'Fam
57 nt
rA
29 nt
3'Cy5
dC
87 nt
E
Lanes
L 19 20 21 22 23 24 25 26 27 L
F
L 28 29 30 31 32 33 34 35 36 L
G
Full length ligation products obtained after RER reconstitution (%)
0
20
40
60
ns
*
rA/dT
rA/dC
Substrate used for RER reconstitution
RER PabPolB
RER PabPolD
RER PabPolB + PabPolD

Figure 2. PabPolB and PabPolD can act in RNase HII-initiated RER pathway

(A–F) (A) Reactions were performed in presence of a dual-labeled matched L87_rA/L87_dT (Table S3) (A–C) or mismatched L87_rA/L87_dC (Table S3) (D–F) rNMP-containing dsDNA template. Reactions were performed in the presence of various combinations of PabPolB, PabPolD, PabFen1, PabPCNA, PabRNase HII and with (B and E) or without (C and F) PabLig1 in buffer containing 1 mM ATP and physiological level of dNTPs as described in STAR methods. Lanes L contain 5′-FAM-labeled oligonucleotide ladders (57- and 87-nt) in FAM panel and 3′-Cy5-labeled oligonucleotide ladders (30- and 87-nt) in Cy5 panel.

(G) Bar graphs representing the means ± standard deviation of full-length ligation products (87-nt) obtained after RER reconstitution with PabPolB (lanes 6, 24) or PabPolD (lanes 7, 25) or both Pols (lanes 8, 26) of at least three independent experiments. p values were determined by unpaired t test and are reported: *p value <0.05 and non-significant (ns). The p values represented above the bars for rA/dC conditions correspond to the difference observed with the same enzyme on the rA/dT substrate.

As observed in Figure 1A, PabRNase HII displayed cleavage activity at the 5′-side of the matched or mismatched rAMP (Figures 2B lane 2; 2E lane 20), leading to the accumulation of 57-nt products in Fam panel (red label) and 30-nt products in Cy5 panel (green label). When PabPolB (Figures 2B lane 3 and 2E lane 21) or PabPolD (Figures 2B lane 4 and 2E lane 22) were supplied in the reaction after PabRNase HII incision, the 3′-OH of the 57-nt strand at the nick was extended to generate full-length extension products (87-nt in length) only detectable in the Fam panel (red label), which was accompanied by the displacement of the 5′-rAMP downstream 30-nt strand (green label; Cy5 panel). Upon addition of PabFen1 and PabLig1, two products (87-nt in length) were detectable in the Fam panel, 5′-end FAM-labeled full-length synthesis products corresponding to the intermediates (red label) obtained by Pol strand-displacement synthesis and double-labeled (5′FAM and 3′Cy5, red and green labels) products (Figures 2B lanes 6–8; 2E lanes 24–26). These 5′FAM and 3′Cy5 dual-labeled fragments migrating at a higher position than the 5′FAM single-labeled full-length synthesis products correspond to the final products of RER reconstitution (ligation products). The efficiency of RER reconstitution is thus assessed by the quantification of double-labeled ligation products observed in Cy5 panels. As such, the total percentage of ligation products was compared between Pols or when Pols are both present, before (Figure 2) or after RNase HII treatment (Figure S2) as described in STAR methods. Interestingly, ligation products obtained without RNase HII treatment (Figures 2B lanes 6–8; 2E lanes 24–26; to see Fam and Cy5 panels) was 48% or 38% with PabPolB (purple bars), 21% or 53% with PabPolD (orange bars), and 30% or 31% with both Pols (gray bars), from a matched or a mismatched rAMP-containing substrate, respectively (Figure 2G). Clearly, these double-labeled ligation products were resistant to RNase HII cleavage (Figures S2B lanes 6–8; S2D lanes 15–17) and their amounts obtained by PabPolB and/or PabPolD-mediated RER were the same as without RNase HII treatment (Figure 2G compared with Figure S2E), indicating that all matched or mismatched rAMP-containing dsDNA templates are efficiently removed by RER. These results show that RER reconstitution with PabPolB or the two Pols displays similar correction efficiencies with either matched or mismatched rAMP-containing dsDNA template, whereas the PabPolD-mediated RER is more active on mismatched than matched rAMP (Figure 2G).

Because RER efficiency slightly differs upon matched and mismatched rAMP depending on the Pol used, we further investigated the prevalence of PolB and PolD in our reconstituted RER assay. Figure S3 shows the influence of one Pol to the other by varying their concentration in the presence of matched (Figures S3A–S3C) or mismatched rAMP-containing dsDNA templates (Figures S3D–S3F), RER enzymes, and physiological concentration of dNTPs. RER was reconstituted either with 250 nM of PabPolB and increasing concentrations of PabPolD (Figures S3C lanes 15–18 and S3F lanes 39–42) or with 1,000 nM of PabPolD and increasing concentrations of PabPolB (Figures S3C lanes 20–23 and S3F lanes 44–47). Products from half of the reaction mixture were submitted to PabRNase HII incubation (Figures S3B and S3E; to see "RNase HII treatment" on top of gels) whereas products from the other half of the reaction mixture were not treated (Figures S3C and S3F; to see "control" on top of gels). This allowed us to ascertain complete removal of embedded rAMP from dsDNA. Double-labeled ligation products treated with PabRNase HII (Figures S3B and S3E) were then quantified in order to evaluate RER efficiencies (Figure S3G). In the presence of a matched or mismatched rAMP-containing dsDNA template, increasing concentrations of PabPolD or PabPolB while keeping the concentration of the other Pol constant generated similar amounts of double-labeled ligation products (Figures S3C lanes 15–18, 20–23 and S3F lanes 39–42, 44–47). Moreover, they were resistant to RNase HII treatment (Figures S3B lanes 3–6, 8–11, S3E lanes 27–30, 32–35), indicating that they were devoid of any embedded rAMP. In these conditions, RER efficiencies were comparable on either matched rA/dT (to compare purple/PolD influence and orange/PolB influence bar graphs in Figure S3G) or mismatched rA/dC (to compare purple/PolD influence and orange/PolB influence bar graphs in Figure S3G), suggesting that PabPolB or PabPolD had no significant effect on each other. On the other hand, RER efficiency was slightly reduced at the highest concentrations of Pols (Figure S3G gray bars). Collectively, these results suggest that both PolD and PolB can support the removal of rNMPs in dsDNA in *Archaea*.

PabFen1 5′-3′ exo/endonuclease activities can act before pols strand displacement in a non-canonical RER pathway

Because we previously showed that PabFen1 5′-3′ exonuclease and 5′-flap endonuclease activities could act after PabRNase HII incision by releasing the 5′-monoribonucleotide on nicked and nicked-flap intermediates (Figure 1C), we sought to confirm that this activity might be relevant in RER. We thus added all enzymes in the reconstitution of the RER pathway except Pols (Figures 2B lane 5 and 2E lane 23). In these conditions, 57-nt products in Fam panel and 30-nt products in Cy5 panel corresponding to PabRNase HII cleavage appeared. In Cy5 panel two other products were also obtained (Figures 2B lane 5 and 2E lane 23), a 29-nt product consistent with 5′-rAMP removal from the 30-nt downstream strand by PabFen1 cleavage activity as observed in Figure 1C (lanes 61–65 and 69–73) and a 31-nt product corresponding to abortive 5′-adenylate intermediate generated by PabLig1 as observed in Figure 1D (lanes 77, 81). Accumulation of ligation failure products (31-nt) corroborates the deficiency of PabLig1 to seal a mismatched rAMP on nicked dsDNA template even in the presence of PabPCNA (Figure 2E lane 23 consistent with results in Figure 1D). However, the sealing of a matched 5′-rAMP stimulated by PabPCNA observed in Figure 1D

is not seen when PabFen1 and PabRNase HII are present in the reaction (Figure 2B lane 5). This result might be explained by the competition between all three proteins to bind with PCNA. Consistently, the lack of detectable interaction between Lig1 and PCNA in cell-free extracts has been previously assigned to multiple PCNA interaction partners.[53] It is also possible that PCNA-interacting proteins display different binding modes on the rA/dT substrate, rendering Lig1 incompetent for nick sealing.[54,55] Interestingly, the 29-nt products corresponding to the removal of the junctional rAMP by PabFen1 were also observed when RER was reconstituted with PabPolD (Figures 2B lane 7 and 2E lane 25, Cy5 panel) but not with PabPolB or both Pols (Figures 2B lanes 6, 8 and 2E lanes 24, 26, Cy5 panel). As such, the signal intensity of the 29-nt product bands remains constant in presence of rA/dT (Figure 2B, lane 5 compared with lane 7, Cy5 panel), while it is slightly reduced in presence of rA/dC (Figure 2E, lane 23 compared with lane 25, Cy5 panel), suggesting that Fen1 cleavage products of mismatched rA/dC are likely resolved by PolD gap filling, followed by DNA ligation.

To confirm that PabFen1 is able to remove the rAMP left behind RNase HII, PabLig1 was omitted in our reconstituted RER (Figures 2C and 2F). As expected, PabFen1 cleavage resulted predominantly in the release of the matched or mismatched rAMP in the absence of PabPols to form 29-nt products (Figures 2C lane 14 and 2F lane 32). These results, consistent with those observed in Figures 2B lane 5 and 2E lane 23, indicate that Fen1 is able to promote either endonucleolytic cleavage of the mismatched rAMP or exonucleolytic cleavage of the fully annealed matched rAMP. The lack of detectable 31-nt products (Figures 2C lane 14 and 2F lane 32, Cy5 panel), which would arise in the presence of PabLig1, confirmed that they were PabLig1-mediated ligation failure products (Figures 2B lane 5 and 2E lane 23, Cy5 panel). The addition of one or the two PabPols in our reconstituted RER lacking PabLig1 resulted in distinct PabFen1 digestion profiles (Figures 2C lane 15–17 and 2F lane 33–35, Cy5 panel). Indeed, on a matched rAMP substrate the coupled activities of PabPolB and PabFen1 generated two major cleavage products of ~27-nt and ~21-nt, corresponding to flap cleavage length ~3-nt and ~9-nt, respectively (Figure 2C lane 15, Cy5 panel). In the reconstituted system lacking PabLig1, the combined activities of PabPolD and PabFen1 gave rise to two main products on both the matched and mismatched rAMP substrates (Figures 2C lane 16 and 2F lane 34, Cy5 panel). Products of 29-nt likely arise because of exonucleolytic cleavage of the fully annealed matched rAMP and, through endonucleolytic cleavage of the mismatched rAMP by PabFen1, as outlined above, while 27-nt products would reflect endonucleolytic cleavage of 3-nt flaps. RER reconstitution with both Pols resulted in a range of cleaved products that differed little from the pattern seen with individual PabPols, except for the 29-nt products that were indistinguishable (Figures 2C lane 17 and 2F lane 35, Cy5 panel). Consistently, the pattern of Fen1 cleavage obtained in our reconstituted RER is the same as previously described.[56] Overall, these results suggest that PabFen1 5′-3′ exonuclease and 5′-flap endonuclease activities may act in RER pathway immediately after PabRNase HII incision, releasing terminal 5′-rNMPs prior to gap filling and ligation.

Functional conservation of RER enzymes among archaeal cells

To confirm that our *in vitro* biochemical reconstitution of functional RER with recombinant enzymes is consistent with their *in vivo* RER requirement and to study the functional conservation of RER enzymes across species, we used or constructed *Thermococcus barophilus* MP (Marteinsson, Birrien and Prieur sp. nov.) (Tba) mutants outlined in Table S1. RER-deficient strains have been shown to grow normally without detectable abnormalities compared to wild-type cells.[32] First, we constructed the heterologous complementation Tba**Δ***polB*::Pab*polB* and Tba**Δ***rnhB*::Pab*rhnB* strains (Table S1) and confirmed that Pab*polB* and Pab*rnhB*, respectively, were expressed in these strains (Figure 3A). Pab*polB* and Pab*rnhB* were overexpressed in Tba**Δ***polB*::Pab*polB* (33-fold) or Tba**Δ***rnhB*::Pab*rnhB* (11-fold), respectively, compared to Tba*polB* and Tba*rnhB* expression in TbaWT (Figure 3A). These overexpressions can be explained by the insertion of ~10 copies of Pab*polB* or Pab*rhnB* in the genomes of Tba**Δ***polB*::Pab*polB* or Tba**Δ***rnhB*::Pab*rhnB*, respectively (see sequencing data). For Tba**Δ***polB*::Pab*polB* the 33-fold overexpression of Pab*polB* may also be due to the difference of promoter strength between Pab and Tba. We also attempted to construct the double-knockout Tba**Δ***rnhB***Δ***polB*, but this leads to synthetic lethality (Table S2). All strains studied exhibited similar growth phenotypes on rich Thermococcales rich medium (TRM) and defined Thermococcales amino acid (TAA) medium (Figures 3B and S4A).

Drop dilution assays were performed to assess the functional conservation of PolB and RNase HII between Pab and Tba (Figure S4B). After exposure to 20 μg/mL MMC, all strains grew normally without any striking difference but none of the strains survived to higher MMC concentrations (Figure S4B). Tba**Δ***polB* was more sensitive to 5 μM 4-Nitroquinoline 1-oxide (4-NQO), 0.1% and 0.2% methyl methane-sulfonate (MMS), and H_2O_2 than TbaWT and Tba**Δ***TERMP_00517*, and the overexpression of Pab*polB* restored the resistance of Tba**Δ***polB*::Pab*polB* to 4-NQO, MMS, and H_2O_2 (Figure S4B) confirming that Tba**Δ***polB* sensitivity to 4-NQO, MMS, and H_2O_2 is due to the loss of PolB. PolB from Pab and Tba share 76.39% amino acid identity, which further supports the functional conservation of PolB in DNA repair. After exposure to MMS, Tba**Δ***rnhB* and Tba**Δ***rnhB*::Pab*rnhB* grew normally in all concentrations tested. The effect of exposure of Tba**Δ***rnhB* to H_2O_2 resulted in reduced survival compared to TbaWT and Tba**Δ***TERMP_00517*, and the overexpression of Pab*rnhB* was not fully restoring the resistance of Tba**Δ***rnhB*::Pab*rnhB* to H_2O_2-induced DNA damage compared to TbaWT (Figure S4B) demonstrating a dominant-negative effect of the overexpression of PabRNase HII in Tba**Δ***rnhB* exposed to H_2O_2. The overexpression of Pab*rnhB* may have an impact on known PCNA interactions,[53] possibly by blocking normal protein interactions in Tba. Consistently, it has been shown that PCNA partners like PolB, Fen1, or Lig1 functionally interact in the repair of oxidative damage in *Thermococcales*.[57] Overall, these results suggest that PabPolB and PabRNase HII proteins can complement several characterized phenotypes in Tba**Δ***polB* and Tba**Δ***rnhB*, respectively, likely indicative of functional conservation of RER enzymes in archaeal species.

Increased accumulation of genomic ribonucleotides in RNase HII and PolB-null Tba cells

To study ribonucleotide presence in genomic DNA, we produced exponentially growing cultures of Tba mutants outlined in Table S1. The level of embedded rNMPs in DNA was analyzed by alkali treatment of genomic DNA causing strand cleavage at incorporated rNMPs,

A

Fold change compared to TbaWT strain		RT-qPCR target	
		PabPolB	PabRNase HII
Strains	TbaΔ*polB*	nd	0.1
	TbaΔ*polB*::Pab*polB*	33.4	1.4
	TbaΔ*rnhB*	0.5	nd
	TbaΔ*rnhB*::Pab*rnhB*	0.2	11.8

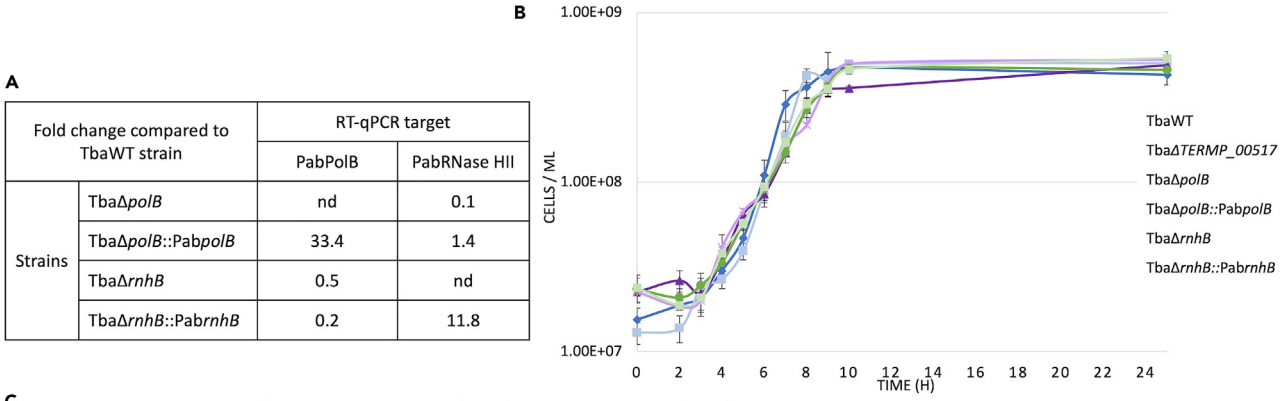

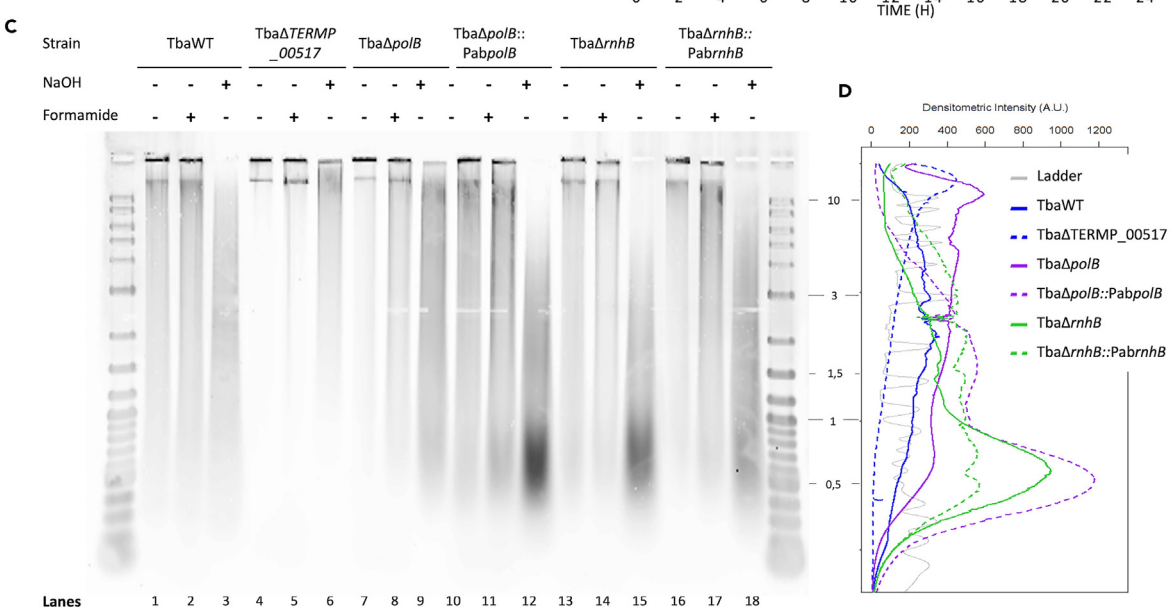

Figure 3. Functional conservation of RER enzymes in *Archaea*

(A) Relative quantification of *polB* and *rnhB* mRNA expression by RT-qPCR in RER mutants (Table S1) compared to TbaWT in at least three independent experiments.

(B) Growth curves of RER mutants in TRM medium. The growth curves are the means ± standard deviation of three independent experiments.

(C) Alkali sensitivity of genomic DNA from RER mutants. Separation by agarose gel of genomic DNA after alkaline (NaOH +) or control treatment with NaCl (NaOH -) under neutral (Formamide -) or denaturing (Formamide +) conditions.

(D) Densitometry traces of NaOH conditions from (C) are shown, and sizes of the DNA markers are indicated on the left.

resulting in an increase of electrophoretic mobility of genomic DNA. DNA mobility of TbaΔ*rnhB* was strongly increased after alkaline treatment compared to TbaWT (Figure 3C lanes 15, 3), giving a substantial shift of densitometry trace (Figure 3D green and blue densitometric continuous lines). These results demonstrate that TbaΔ*rnhB* accumulated more genomic rNMPs than TbaWT, which on average leads to ∼1 rNMP every 700 bp. Interestingly, DNA mobility of TbaΔ*rnhB*::Pab*rhnB* was almost similar to that of TbaWT (Figure 3C lanes 18 and 3), giving rise to similar densitometry traces (Figure 3D densitometric green dashed and blue continuous lines). This result was quite intriguing since it did not reflect the overexpression of Pab*rhnB* in TbaΔ*rnhB* (Figure 3A). This could indicate that the overexpression of PabRNase HII does not improve the correction of genomic rNMPs in TbaΔ*rnhB* compared to basal TbaRNase HII expression in TbaWT. The slight increase of DNA fragmentation in TbaΔ*rnhB*::Pab*rhnB* could also be due to an increase of other DNA lesions or the presence of embedded rNMPs in inaccessible regions for RNase HII (e.g., secondary structures). Nonetheless, these results show that PabRNase HII can replace RER functions of TbaRNase HII in Tba. This finding is thus consistent with the *in vitro* biochemical activities of PabRNase HII described in Figure 1A and its requirement for initiating RER observed in Figure 2. The mobility of DNA fragments after alkaline treatment for TbaΔ*polB* genomic DNA with respect to TbaWT was barely increased (Figures 3C lanes 9, 3 and 3D densitometric purple and blue continuous lines) but obviously not comparable to that of Tba*ΔrnhB* (Figure 3C lanes 9 and 15). Surprisingly, DNA mobility of TbaΔ*polB*::Pab*polB* was increased after alkaline treatment (Figure 3C lanes 12, 11), giving a substantial densitometry peak shift with respect to TbaΔ*polB* (Figure 3D densitometric purple dashed and continuous lines). The estimated incorporation frequency of ∼1 rNMP every 800 bp in TbaΔ*polB*::Pab*polB* DNA indicates a

high level of rNMPs retention compared to TbaWT and Tba*ΔpolB* (Figure 3C, lanes 12 compared with lanes 3 and 9). This indicates that the overexpression of PabPolB in Tba displays a higher frequency of rNMP incorporation or/and inserts more alkali-labile DNA damages compared to TbaWT. In our previous study,[2] a higher frequency of rNMP incorporation in Pab genome was detectable compare to Tba, perhaps suggesting a higher propensity of rNMPs or alkali-labile damages incorporation by Pols. Sharing 76.39% amino acid identity, TbaPolB and PabPolB might display different rNMP incorporation frequency, like that observed between PabPolB and PolB from *Thermococcus kodakarensis*.[1] TkoPolB seems to have a higher capacity for rNMP incorporation in DNA than PabPolB as previously outlined.[2] The overexpression of PabPolB could also counteract the activity of the physiological TbaPolB or disrupt the interactions with other RER enzymes leading to an inefficient correction of rNMPs by RER. Taken together, these results suggest that RNase HII can initiate the repair of genomic rNMPs and that PolB, or another Pol, like PolD, may be involved in RER. Furthermore, it appears that RNase HII-mediated rNMP removal can only remove parts of the incorporated rNMPs in the genome, questioning about the chemical identity of the retained rNMPs and their physiological consequences.

DISCUSSION

There are growing *in vitro* studies showing that mismatched rNMPs may be generated by Pols either by inserting incorrect rNMP opposite template DNA base or by incorporating incorrect dNMP opposite unrepaired template RNA base.[2,36–38] However, it is presently not known to what extent mismatched rNMPs are repaired by RNase HII-initiated RER. Here, we demonstrate that the RER pathway may be involved in their removal *in vitro*, using model substrates and RER enzymes (RNase HII, Pol, Lig1, Fen1) from *P. abyssi*. Functionally homologous to the eukaryotic counterpart,[31] PabRNase HII is able to specifically cleave at the 5′-side of a mismatched rAMP (rA/dC). We observed that PabRNase HII activity was less efficient on an rG/dA mismatch compared with the rA/dC mismatch. The weak incision of rG/dA mismatch by PabRNase HII in agreement with previous results[31] suggests that PabRNase HII incision activity is likely influenced by the identity of the mismatched rNMP base pair in DNA. To further analyze the substrate spectrum of PabRNase HII, it would be interesting to measure the differential cleavage activity of PabRNase HII on all twelve possibilities of rNMP-mismatched base pairs in the same reaction conditions. *In vivo* analyses confirm our previous findings that deleting *rnhB* from Tba induces the accumulation of genomic rNMPs in comparison with TbaWT.[2] The overexpression of Pab*rnhB*, sharing 63.18% amino acid identity with Tba*rnhB*, in Tba*ΔrnhB* restores the genomic rNMP incorporation frequency to the TbaWT level. However, overexpression of Pab*rnhB* does not further reduce the numbers of rNMPs in DNA, highlighting a baseline of rNMP or other DNA lesions (e.g., abasic sites) retention in the genome of exponentially growing *Archaea*. Retained rNMPs in the genomes might represent DNA repair hallmarks presumably beneficial for archaeal cells.

In the RER pathway on matched rNMPs, the RNase HII/2-dependent cleavage is followed by strand-displacement synthesis by Pol.[20,21,34] Consistent with the previous archaeal study on matched rNMPs,[1] we demonstrate that RER is more efficient with PolB compared to PolD. However, RER with both PolB and PolD does not correct as many embedded rNMP as RER with PolB alone but instead is less efficient. The observed difference of Pol-mediated RER efficiencies is likely relevant to the identity of rNMP base pairs (rA/dT versus rG/dC), the sequence of the downstream strand and dNTP concentrations (Pab cellular dNTP concentrations versus 0.1 mM dNTPs in Heider et al.[1]). In yeast, both Polδ and Polε can also act in RER, but RER with Polδ is two times more efficient than RER with Polε.[20] In *E. coli*, Pol I could be substituted by Pol III in RER.[21] Therefore, the redundancy for Pol activities in RER on matched rNMPs seems to be conserved in all domains of life. Not yet addressed in eukaryotes and *Bacteria*, mismatched RER studies are now awaited. Here, we demonstrate that archaeal RER with PolB is as efficient to correct a matched rNMP as it is to correct a mismatched rNMP whereas RER with PolD was more efficient to correct a mismatched than a matched rNMP. The presence of 5′-mismatched rNMPs in the downstream strand appears to enhance PolD strand-displacement activity compared to the refractory effect of matched rNMPs. Of particular importance, the 3′-proofreading exonuclease function in PolD and PolB, known to impede strand displacement, was inactivated in order to prevent releasing of the Cy5 fluorescent label. Therefore, PolD strand-displacement activity of the downstream rNMP-containing strand fully annealed to DNA template is relatively weak compared to PolB, which is in general agreement with previous results.[56,58,59] The efficiency of RER with PolD in our model is thus potentially overestimated due to the inactivation of the exonuclease function. However, the knockout of PolB *in vivo* displays only a slight increase of genomic rNMPs, suggesting that an alternate enzyme, likely PolD, may compensate for PolB deficiency in RER, consistent with our *in vitro* RER reconstitution.

Interestingly, our *in vitro* RER reconstitution assay reveals that PabFen1 can also remove the 5′-terminal rNMP after PabRNase HII incision but before extension by Pol. Product intermediates corresponding to Fen1 cleavage 3′ to the rAMP were only detectable in the PolD-mediated RER pathway. This indicates that failure to carry out strand-displacement synthesis by PolD may promote the removal of the 5′-terminal rNMP by Fen1 as a backup pathway for RER. Generally, the results are consistent with those obtained by Fen1 nuclease activity on RNase HII-like RER substrates. Both mismatched and matched rNMPs are efficiently removed by PabFen1 5′-3′ exo/endonuclease activity, while showing a slightly reduction in the presence of 5′-terminal dNMP. PabFen1, being a structure-dependent and evolutionary conserved nuclease,[45,60,61] may utilize a less-efficient substrate recognition mode or/and bind differently the rAMP-substrate structure, perhaps by altering the specific interaction sites of amino acids residues on the sugar of the terminal nucleotide. It has been observed that human and yeast Fen1 exonuclease activity can excise a ribonucleotide after RNase HII incision in the context of Okazaki fragment processing,[40,42] but only two studies[5,62] suggest that the combination of Fen1 and RNase HII rNMP cleavage could potentially act to repair single embedded rNMPs in DNA. In yeast, the exonuclease Exo1 is thought to replace Fen1 for flap cleavage in the RER pathway although RER with Exo1 is less efficient than RER with Fen1.[20] This model seems to be consistent with previous *in vivo* and *in vitro* functional evidences of Exo1.[63] More recently, it has been proposed that an RNase H2- and Exo1-mediated exonucleolytic pathway is involved in RNA-DNA primer removal of Okazaki fragments in eukaryotic cells,[41] reinforcing the possibility of single embedded rNMP removal by Fen1 in eukaryotes. In *Bacteria*, after RNase HII incision,

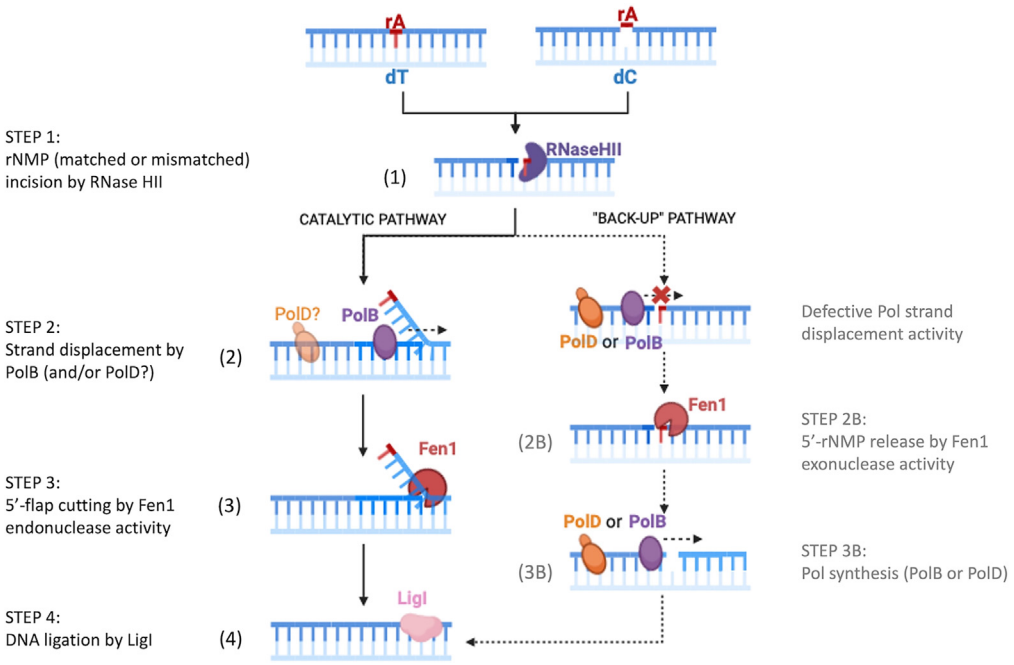

Figure 4. Proposed RER model for matched or mismatched rNMP removal in *Archaea*

The archaeal RER pathway is efficient to repair matched (rA/dT) or mismatched (rA/dC) rNMP-containing dsDNA. STEP 1 involves the incision at the 5′-side of the matched or mismatched embedded rNMP by RNase HII. In the canonical RER pathway, STEP 2 implies strand-displacement synthesis mainly by PolB creating the 5′-terminal rNMP-containing flap subsequently cut by Fen1 endonuclease activity in STEP 3. PolD might replace PolB in STEP 2 for strand-displacement synthesis of mismatched 5′-rNMP-containing flap. In case of defective strand-displacement activity by Pol, Fen1 5′-3′ exonuclease or 5′-flap endonuclease activity could release the 5′-terminal rNMP after RNase HII incision (STEP 2B) but before PolB or PolD extension in STEP 3B. STEP 4 involves the sealing by Lig1 of DNA ends. Schematic illustrations are created with Biorender (https://biorender.com).

Pol I cuts the rNMP either by 5′-flap endonuclease activity or by 5′-3′ exonuclease activity.[21] Based on this evidence, we suggest that RNase HII/2- and Fen1-mediated exonucleolytic and endonucleolytic processing of single embedded rNMPs in DNA is relevant to *Archaea* and possibly applies to eukaryotes and *Bacteria*.

On the other hand, we demonstrate that the presence of matched rNMP intermediates is refractory to nick sealing in the absence of PabPCNA and PabLig1 undergoes abortive ligation, similar to what happens with eukaryotic DNA ligases I and III on 5′-rNMP nicked substrates.[5,49] Fortunately, ligation failure products that contain 5′-AMP adducts are resolved by Aprataxin to ensure genome integrity in eukaryotes.[49] Despite conserved DNA metabolisms and common protein structural homologies with eukaryotes, there is no functional equivalent in *Archaea*. Nonetheless, PabPCNA triggers end-joining of 5′-matched rNMP or 5′-mismatched dNMP structures by PabLig1, but only slightly for mismatched rNMPs in our experimental conditions. We suggest that the functional interaction between PCNA and Lig1 is perturbed on mismatched rNMPs, leading to the formation of an unstable PCNA-Lig1 complex. A previous study revealed that at least two binding sites on PabLig1 are required for efficient PCNA binding.[53] Therefore, we hypothesize that these PCNA-ligase interaction strengths are disturbed on the rA/dC mismatch possibly due to the ribose sugar and that conformational switching required for efficient ligation is not reached.[53,55]

Overall, our data allow us to propose a model for matched and mismatched RER pathway (Figure 4). The RER mechanism relies on the initial RNase HII incision at the 5′-side of matched or mismatched rNMP (Figure 4 step 1), followed by extension and strand-displacement synthesis by Pol (Figure 4 step 2). The resulting flap is cut by Fen1 endonuclease activity (Figure 4 step 3), which creates a ligatable nick for DNA ligase 1. Then Lig1 seals nicked structures to finalize repair (Figure 4 step 4). Because of robust strand-displacement DNA synthesis by PolB on 5-′rNMP nicked templates, PolB seems to be the main Pol involved in RER. However, our *in vivo* and *in vitro* data suggest than in absence of PolB, PolD could act in a less-efficient RER. On the other hand, we propose that defects in strand-displacement DNA synthesis by Pol (e.g., flawed mutant Pol, presence of template damage or unfavorable sequence contexts) disengage a backup RER pathway, in which Fen1 exonuclease activity removes the 5′ terminal rNMP after PabRNase HII incision (Figure 4 step 2B) before 1-nt gap filling by Pol (Figure 4 step 3B).

Limitations of the study

In this study, we demonstrate that the type 2 RNase H (RNase HII/2) RER pathway is functional *in vitro* to remove mispaired rNMPs in DNA. We found that RNase HII, DNA Pol, Lig1, and Fen1 from *Pyrococcus abyssi* can incise, excise, and process rA/dC, a mispair generated by erroneous insertion of the replicative family D DNA polymerase *in vitro*. However, RER reconstitution was restricted to rA/dC mispair. Thus, it would be interesting to expand the study to other relevant PolD-mediated mispair rNMP insertions. Moreover, it was not possible to correlate

in vitro RER efficiency on mispaired rNMPs with their occurrence in genomic DNA. Finally, we show that a backup RNase HII/2 RER pathway can process paired and mispaired rNMPs *in vitro* due to defective strand-displacement activity by DNA Pol. However, the interplay between the primary and backup RER pathway remains to be fully addressed *in vivo*.

STAR★METHODS

Detailed methods are provided in the online version of this paper and include the following:

- KEY RESOURCES TABLE
- RESOURCE AVAILABILITY
  - Lead contact
  - Material availability
  - Data and code availability
- EXPERIMENTAL MODEL AND STUDY PARTICIPANT DETAILS
- METHOD DETAILS
  - Enzymes production and purification
  - Oligonucleotides
  - RNase HII, PolB, PolD, Fen1 and Lig1 activity assays
  - *In vitro* RER reconstitution
  - RNA isolation and qRT-PCR analysis
  - Detection of ribonucleotides in genomic DNA
  - Drop dilution assays
- QUANTIFICATION AND STATISTICAL ANALYSIS
  - Visualisation and quantification of fluorescently labelled products
  - RNA isolation and qRT-PCR analysis
  - Detection of ribonucleotides in genomic DNA

SUPPLEMENTAL INFORMATION

Supplemental information can be found online at https://doi.org/10.1016/j.isci.2023.108479.

ACKNOWLEDGMENTS

M.R. was financially supported by IFREMER and the Brittany Regional Council. This work has received funding from the French Institute of Marine Research and Exploitation (IFREMER).

AUTHOR CONTRIBUTIONS

Conceptualization, M.R., Y.M., M.J., and G.H.; methodology, M.R., A.B., L.V., R.B., Y.M., and G.H.; investigation, M.R., L.C., B.V., A.B., L.V., R.B., Y.M., and G.H.; validation, M.R., L.V., Y.M., M.J., and G.H.; data curation, M.R., A.B., Y.M., and G.H.; supervision, Y.M., M.J., and G.H.; funding acquisition, G.H.; project administration, M.R. and G.H.; writing - review & editing, M.R. and G.H.

DECLARATION OF INTERESTS

The authors declare no competing interests.

Received: July 11, 2023
Revised: October 5, 2023
Accepted: November 14, 2023
Published: November 17, 2023

REFERENCES

1. Heider, M.R., Burkhart, B.W., Santangelo, T.J., and Gardner, A.F. (2017). Defining the RNaseH2 enzyme-initiated ribonucleotide excision repair pathway in *Archaea*. J. Biol. Chem. *292*, 8835–8845.
2. Lemor, M., Kong, Z., Henry, E., Brizard, R., Laurent, S., Bossé, A., and Henneke, G. (2018). Differential Activities of DNA Polymerases in Processing Ribonucleotides during DNA Synthesis in *Archaea*. J. Mol. Biol. *430*, 4908–4924.
3. Nick McElhinny, S.A., Watts, B.E., Kumar, D., Watt, D.L., Lundström, E.B., Burgers, P.M.J., Johansson, E., Chabes, A., and Kunkel, T.A. (2010). Abundant ribonucleotide incorporation into DNA by yeast replicative polymerases. Proc. Natl. Acad. Sci. USA *107*, 4949–4954.
4. Yao, N.Y., Schroeder, J.W., Yurieva, O., Simmons, L.A., and O'Donnell, M.E. (2013). Cost of rNTP/dNTP pool imbalance at the replication fork. Proc. Natl. Acad. Sci. USA *110*, 12942–12947.
5. Rumbaugh, J.A., Murante, R.S., Shi, S., and Bambara, R.A. (1997). Creation and removal of embedded ribonucleotides in chromosomal DNA during mammalian Okazaki fragment processing. J. Biol. Chem. *272*, 22591–22599.
6. Zheng, L., and Shen, B. (2011). Okazaki fragment maturation: nucleases take centre stage. J. Mol. Cell Biol. *3*, 23–30.

7. Randerath, K., Reddy, R., Danna, T.F., Watson, W.P., Crane, A.E., and Randerath, E. (1992). Formation of ribonucleotides in DNA modified by oxidative damage *in vitro* and *in vivo*. Characterization by 32P-postlabeling. Mutat. Res. *275*, 355–366.
8. Vengrova, S., and Dalgaard, J.Z. (2004). RNase-sensitive DNA modification(s) initiates *S. pombe* mating-type switching. Genes Dev. *18*, 794–804.
9. Vengrova, S., and Dalgaard, J.Z. (2006). The wild-type *Schizosaccharomyces pombe* mat1 imprint consists of two ribonucleotides. EMBO Rep. *7*, 59–65.
10. Evich, M., Spring-Connell, A.M., Storici, F., and Germann, M.W. (2016). Structural Impact of Single Ribonucleotide Residues in DNA. Chembiochem *17*, 1968–1977.
11. Klein, H.L. (2017). Genome instabilities arising from ribonucleotides in DNA. DNA Repair *56*, 26–32.
12. Nick McElhinny, S.A., Kumar, D., Clark, A.B., Watt, D.L., Watts, B.E., Lundström, E.B., Johansson, E., Chabes, A., and Kunkel, T.A. (2010). Genome instability due to ribonucleotide incorporation into DNA. Nat. Chem. Biol. *6*, 774–781.
13. Pizzi, S., Sertic, S., Orcesi, S., Cereda, C., Bianchi, M., Jackson, A.P., Lazzaro, F., Plevani, P., and Muzi-Falconi, M. (2015). Reduction of hRNase H2 activity in Aicardi-Goutieres syndrome cells leads to replication stress and genome instability. Hum. Mol. Genet. *24*, 649–658.
14. Reijns, M.A.M., Rabe, B., Rigby, R.E., Mill, P., Astell, K.R., Lettice, L.A., Boyle, S., Leitch, A., Keighren, M., Kilanowski, F., et al. (2012). Enzymatic removal of ribonucleotides from DNA is essential for mammalian genome integrity and development. Cell *149*, 1008–1022.
15. Crow, Y.J., Leitch, A., Hayward, B.E., Garner, A., Parmar, R., Griffith, E., Ali, M., Semple, C., Aicardi, J., Babul-Hirji, R., et al. (2006). Mutations in genes encoding ribonuclease H2 subunits cause Aicardi-Goutieres syndrome and mimic congenital viral brain infection. Nat. Genet. *38*, 910–916.
16. Günther, C., Kind, B., Reijns, M.A.M., Berndt, N., Martinez-Bueno, M., Wolf, C., Tüngler, V., Chara, O., Lee, Y.A., Hübner, N., et al. (2015). Defective removal of ribonucleotides from DNA promotes systemic autoimmunity. J. Clin. Invest. *125*, 413–424.
17. Aden, K., Bartsch, K., Dahl, J., Reijns, M.A.M., Esser, D., Sheibani-Tezerji, R., Sinha, A., Wottawa, F., Ito, G., Mishra, N., et al. (2019). Epithelial RNase H2 Maintains Genome Integrity and Prevents Intestinal Tumorigenesis in Mice. Gastroenterology *156*, 145–159.e19.
18. Hiller, B., Achleitner, M., Glage, S., Naumann, R., Behrendt, R., and Roers, A. (2012). Mammalian RNase H2 removes ribonucleotides from DNA to maintain genome integrity. J. Exp. Med. *209*, 1419–1426.
19. Uehara, R., Cerritelli, S.M., Hasin, N., Sakhuja, K., London, M., Iranzo, J., Chon, H., Grinberg, A., and Crouch, R.J. (2018). Two RNase H2 Mutants with Differential rNMP Processing Activity Reveal a Threshold of Ribonucleotide Tolerance for Embryonic Development. Cell Rep. *25*, 1135–1145.e5.
20. Sparks, J.L., Chon, H., Cerritelli, S.M., Kunkel, T.A., Johansson, E., Crouch, R.J., and Burgers, P.M. (2012). RNase H2-initiated ribonucleotide excision repair. Mol. Cell *47*, 980–986.
21. Vaisman, A., McDonald, J.P., Noll, S., Huston, D., Loeb, G., Goodman, M.F., and Woodgate, R. (2014). Investigating the mechanisms of ribonucleotide excision repair in *Escherichia coli*. Mutat. Res. *761*, 21–33.
22. Cerritelli, S.M., Iranzo, J., Sharma, S., Chabes, A., Crouch, R.J., Tollervey, D., and El Hage, A. (2020). High density of unrepaired genomic ribonucleotides leads to Topoisomerase 1-mediated severe growth defects in absence of ribonucleotide reductase. Nucleic Acids Res. *48*, 4274–4297.
23. Kim, N., Huang, S.Y.N., Williams, J.S., Li, Y.C., Clark, A.B., Cho, J.E., Kunkel, T.A., Pommier, Y., and Jinks-Robertson, S. (2011). Mutagenic processing of ribonucleotides in DNA by yeast topoisomerase I. Science *332*, 1561–1564.
24. Reijns, M.A.M., Parry, D.A., Williams, T.C., Nadeu, F., Hindshaw, R.L., Rios Szwed, D.O., Nicholson, M.D., Carroll, P., Boyle, S., Royo, R., et al. (2022). Signatures of TOP1 transcription-associated mutagenesis in cancer and germline. Nature *602*, 623–631.
25. Sparks, J.L., and Burgers, P.M. (2015). Error-free and mutagenic processing of topoisomerase 1-provoked damage at genomic ribonucleotides. EMBO J. *34*, 1259–1269.
26. Williams, J.S., Smith, D.J., Marjavaara, L., Lujan, S.A., Chabes, A., and Kunkel, T.A. (2013). Topoisomerase 1-mediated removal of ribonucleotides from nascent leading-strand DNA. Mol. Cell *49*, 1010–1015.
27. Malfatti, M.C., Balachander, S., Antoniali, G., Koh, K.D., Saint-Pierre, C., Gasparutto, D., Chon, H., Crouch, R.J., Storici, F., and Tell, G. (2017). Abasic and oxidized ribonucleotides embedded in DNA are processed by human APE1 and not by RNase H2. Nucleic Acids Res. *45*, 11193–11212.
28. Vaisman, A., McDonald, J.P., Huston, D., Kuban, W., Liu, L., Van Houten, B., and Woodgate, R. (2013). Removal of misincorporated ribonucleotides from prokaryotic genomes: an unexpected role for nucleotide excision repair. PLoS Genet. *9*, e1003878.
29. Shen, Y., Koh, K.D., Weiss, B., and Storici, F. (2011). Mispaired rNMPs in DNA are mutagenic and are targets of mismatch repair and RNases H. Nat. Struct. Mol. Biol. *19*, 98–104.
30. Chon, H., Sparks, J.L., Rychlik, M., Nowotny, M., Burgers, P.M., Crouch, R.J., and Cerritelli, S.M. (2013). RNase H2 roles in genome integrity revealed by unlinking its activities. Nucleic Acids Res. *41*, 3130–3143.
31. Malfatti, M.C., Henneke, G., Balachander, S., Koh, K.D., Newnam, G., Uehara, R., Crouch, R.J., Storici, F., and Tell, G. (2019). Unlike the *Escherichia coli* counterpart, archaeal RNase HII cannot process ribose monophosphate abasic sites and oxidized ribonucleotides embedded in DNA. J. Biol. Chem. *294*, 13061–13072.
32. Birien, T., Thiel, A., Henneke, G., Flament, D., Moalic, Y., and Jebbar, M. (2018). Development of an Effective 6-Methylpurine Counterselection Marker for Genetic Manipulation in *Thermococcus barophilus*. Genes *9*, 77.
33. Burkhart, B.W., Cubonova, L., Heider, M.R., Kelman, Z., Reeve, J.N., and Santangelo, T.J. (2017). The GAN Exonuclease or the Flap Endonuclease Fen1 and RNase HII Are Necessary for Viability of *Thermococcus kodakarensis*. J. Bacteriol. *199*, e00141-17.
34. Randall, J.R., Nye, T.M., Wozniak, K.J., and Simmons, L.A. (2019). RNase HIII Is Important for Okazaki Fragment Processing in *Bacillus subtilis*. J. Bacteriol. *201*, e00686-18.
35. Dede, M., Napolitano, S., Melati, A., Pirota, V., Maga, G., and Crespan, E. (2021). High Flexibility of RNaseH2 Catalytic Activity with Respect to Non-Canonical DNA Structures. Int. J. Mol. Sci. *22*, 5201.
36. Ordonez, H., Uson, M.L., and Shuman, S. (2014). Characterization of three mycobacterial DinB (DNA polymerase IV) paralogs highlights DinB2 as naturally adept at ribonucleotide incorporation. Nucleic Acids Res. *42*, 11056–11070.
37. Cilli, P., Minoprio, A., Bossa, C., Bignami, M., and Mazzei, F. (2015). Formation and Repair of Mismatches Containing Ribonucleotides and Oxidized Bases at Repeated DNA Sequences. J. Biol. Chem. *290*, 26259–26269.
38. Jamsen, J.A., Sassa, A., Perera, L., Shock, D.D., Beard, W.A., and Wilson, S.H. (2021). Structural basis for proficient oxidized ribonucleotide insertion in double strand break repair. Nat. Commun. *12*, 5055.
39. Williams, J.S., Lujan, S.A., and Kunkel, T.A. (2016). Processing ribonucleotides incorporated during eukaryotic DNA replication. Nat. Rev. Mol. Cell Biol. *17*, 350–363.
40. Huang, L., Rumbaugh, J.A., Murante, R.S., Lin, R.J., Rust, L., and Bambara, R.A. (1996). Role of calf RTH-1 nuclease in removal of 5′-ribonucleotides during Okazaki fragment processing. Biochemistry *35*, 9266–9277.
41. Liu, B., Hu, J., Wang, J., and Kong, D. (2017). Direct Visualization of RNA-DNA Primer Removal from Okazaki Fragments Provides Support for Flap Cleavage and Exonucleolytic Pathways in Eukaryotic Cells. J. Biol. Chem. *292*, 4777–4788.
42. Sato, A., Kanai, A., Itaya, M., and Tomita, M. (2003). Cooperative regulation for Okazaki fragment processing by RNase HII and FEN-1 purified from a hyperthermophilic archaeon, *Pyrococcus furiosus*. Biochem. Biophys. Res. Commun. *309*, 247–252.
43. Kao, H.I., Henricksen, L.A., Liu, Y., and Bambara, R.A. (2002). Cleavage specificity of *Saccharomyces cerevisiae* flap endonuclease 1 suggests a double-flap structure as the cellular substrate. J. Biol. Chem. *277*, 14379–14389.
44. Matsui, E., Urushibata, Y., Abe, J., and Matsui, I. (2014). Serial intermediates with a 1 nt 3′-flap and 5′ variable-length flaps are formed by cooperative functioning of *Pyrococcus horikoshii* FEN-1 with either B or D DNA polymerases. Extremophiles *18*, 415–427.
45. Friedrich-Heineken, E., and Hübscher, U. (2004). The Fen1 extrahelical 3′-flap pocket is conserved from *Archaea* to human and regulates DNA substrate specificity. Nucleic Acids Res. *32*, 2520–2528.
46. Harrington, J.J., and Lieber, M.R. (1995). DNA structural elements required for FEN-1 binding. J. Biol. Chem. *270*, 4503–4508.
47. Friedrich-Heineken, E., Henneke, G., Ferrari, E., and Hübscher, U. (2003). The acetylatable lysines of human Fen1 are important for endo- and exonuclease activities. J. Mol. Biol. *328*, 73–84.
48. Tomkinson, A.E., and Levin, D.S. (1997). Mammalian DNA ligases. Bioessays *19*, 893–901.
49. Tumbale, P., Williams, J.S., Schellenberg, M.J., Kunkel, T.A., and Williams, R.S. (2014). Aprataxin resolves adenylated RNA-DNA

junctions to maintain genome integrity. Nature *506*, 111–115.
50. Yang, S.W., and Chan, J.Y. (1992). Analysis of the formation of AMP-DNA intermediate and the successive reaction by human DNA ligases I and II. J. Biol. Chem. *267*, 8117–8122.
51. Zhu, H., and Shuman, S. (2008). Bacterial nonhomologous end joining ligases preferentially seal breaks with a 3′-OH monoribonucleotide. J. Biol. Chem. *283*, 8331–8339.
52. Killelea, T., Palud, A., Akcha, F., Lemor, M., L'Haridon, S., Godfroy, A., and Henneke, G. (2019). The interplay at the replisome mitigates the impact of oxidative damage on the genetic integrity of hyperthermophilic *Archaea*. Elife *8*, 45320.
53. Meslet-Cladiére, L., Norais, C., Kuhn, J., Briffotaux, J., Sloostra, J.W., Ferrari, E., Hübscher, U., Flament, D., and Myllykallio, H. (2007). A novel proteomic approach identifies new interaction partners for proliferating cell nuclear antigen. J. Mol. Biol. *372*, 1137–1148.
54. Gomes, X.V., and Burgers, P.M. (2000). Two modes of FEN1 binding to PCNA regulated by DNA. EMBO J. *19*, 3811–3821.
55. Pascal, J.M., Tsodikov, O.V., Hura, G.L., Song, W., Cotner, E.A., Classen, S., Tomkinson, A.E., Tainer, J.A., and Ellenberger, T. (2006). A flexible interface between DNA ligase and PCNA supports conformational switching and efficient ligation of DNA. Mol. Cell *24*, 279–291.
56. Henneke, G. (2012). *In vitro* reconstitution of RNA primer removal in *Archaea* reveals the existence of two pathways. Biochem. J. *447*, 271–280.
57. Gehring, A.M., Zatopek, K.M., Burkhart, B.W., Potapov, V., Santangelo, T.J., and Gardner, A.F. (2020). Biochemical reconstitution and genetic characterization of the major oxidative damage base excision DNA repair pathway in *Thermococcus kodakarensis*. DNA Repair *86*, 102767.
58. Greenough, L., Kelman, Z., and Gardner, A.F. (2015). The roles of family B and D DNA polymerases in *Thermococcus* species 9 degrees N Okazaki fragment maturation. J. Biol. Chem. *290*, 12514–12522.
59. Hogrel, G., Lu, Y., Alexandre, N., Bossé, A., Dulermo, R., Ishino, S., Ishino, Y., and Flament, D. (2020). Role of RadA and DNA Polymerases in Recombination-Associated DNA Synthesis in Hyperthermophilic *Archaea*. Biomolecules *10*, 1045.
60. Qiu, J., Liu, R., Chapados, B.R., Sherman, M., Tainer, J.A., and Shen, B. (2004). Interaction interface of human flap endonuclease-1 with its DNA substrates. J. Biol. Chem. *279*, 24394–24402.
61. Liu, R., Qiu, J., Finger, L.D., Zheng, L., and Shen, B. (2006). The DNA-protein interaction modes of FEN-1 with gap substrates and their implication in preventing duplication mutations. Nucleic Acids Res. *34*, 1772–1784.
62. Rydberg, B., and Game, J. (2002). Excision of misincorporated ribonucleotides in DNA by RNase H (type 2) and FEN-1 in cell-free extracts. Proc. Natl. Acad. Sci. USA *99*, 16654–16659.
63. Tran, P.T., Erdeniz, N., Dudley, S., and Liskay, R.M. (2002). Characterization of nuclease-dependent functions of Exo1p in *Saccharomyces cerevisiae*. DNA Repair *1*, 895–912.
64. Gouge, J., Ralec, C., Henneke, G., and Delarue, M. (2012). Molecular recognition of canonical and deaminated bases by *P. abyssi* family B DNA polymerase. J. Mol. Biol. *423*, 315–336.
65. Palud, A., Villani, G., L'Haridon, S., Querellou, J., Raffin, J.P., and Henneke, G. (2008). Intrinsic properties of the two replicative DNA polymerases of *Pyrococcus abyssi* in replicating abasic sites: possible role in DNA damage tolerance? Mol. Microbiol. *70*, 746–761.
66. Zeng, X., Birrien, J.L., Fouquet, Y., Cherkashov, G., Jebbar, M., Querellou, J., Oger, P., Cambon-Bonavita, M.A., Xiao, X., and Prieur, D. (2009). *Pyrococcus* CH1, an obligate piezophilic hyperthermophile: extending the upper pressure-temperature limits for life. ISME J. *3*, 873–876.
67. Thiel, A., Michoud, G., Moalic, Y., Flament, D., and Jebbar, M. (2014). Genetic manipulations of the hyperthermophilic piezophilic archaeon *Thermococcus barophilus*. Appl. Environ. Microbiol. *80*, 2299–2306.
68. Godfroy, A., Raven, N.D., and Sharp, R.J. (2000). Physiology and continuous culture of the hyperthermophilic deep-sea vent archaeon *Pyrococcus abyssi* ST549. FEMS Microbiol. Lett. *186*, 127–132.
69. Raven, N., Ladwa, N., Cossar, D., and Sharp, R. (1992). Continuous Culture of the Hyperthermophilic Archaeum-Asterisk *Pyrococcus furiosus*. Appl Microbiol Biot *38*, 263–267.
70. Raven, N.D., and Sharp, R.J. (2006). Development of defined and minimal media for the growth of the hyperthermophilic archaeon *Pyrococcus furiosus* Vc1. FEMS Microbiol. Lett. *146*, 135–141.
71. Henneke, G., Gueguen, Y., Flament, D., Azam, P., Querellou, J., Dietrich, J., Hübscher, U., and Raffin, J.P. (2002). Replication factor C from the hyperthermophilic archaeon *Pyrococcus abyssi* does not need ATP hydrolysis for clamp-loading and contains a functionally conserved RFC PCNA-binding domain. J. Mol. Biol. *323*, 795–810.
72. Carre, L., Henneke, G., Henry, E., Flament, D., Girard, E., and Bruno, F. (2023). DNA Polymerization in Icy Moon Abyssal Pressure Conditions. Astrobiology *1*.
73. Ding, J., Taylor, M.S., Jackson, A.P., and Reijns, M.A.M. (2015). Genome-wide mapping of embedded ribonucleotides and other noncanonical nucleotides using emRiboSeq and EndoSeq. Nat. Protoc. *10*, 1433–1444.
74. Ramírez, M., Velázquez, R., Maqueda, M., López-Piñeiro, A., and Ribas, J.C. (2015). A new wine *Torulaspora delbrueckii* killer strain with broad antifungal activity and its toxin-encoding double-stranded RNA virus. Front. Microbiol. *6*, 983.
75. Fujikane, R., Ishino, S., Ishino, Y., and Forterre, P. (2010). Genetic analysis of DNA repair in the hyperthermophilic archaeon, *Thermococcus kodakaraensis*. Genes Genet. Syst. *85*, 243–257.
76. Kushida, T., Narumi, I., Ishino, S., Ishino, Y., Fujiwara, S., Imanaka, T., and Higashibata, H. (2019). Pol B, a Family B DNA Polymerase, in *Thermococcus kodakarensis* is Important for DNA Repair, but not DNA Replication. Microbes Environ. *34*, 316–326.
77. Schmittgen, T.D., and Livak, K.J. (2008). Analyzing real-time PCR data by the comparative C-T method. Nat. Protoc. *3*, 1101–1108.

STAR★METHODS

KEY RESOURCES TABLE

REAGENT or RESOURCE	SOURCE	IDENTIFIER
Bacterial and virus strains		
E. coli DH5α (4 x 500 μL)	ThermoFisher Scientific	18265017
Chemicals, peptides, and recombinant proteins		
Pab PolB (D215A mutation)	Gouge et al., 2012[64]	
Pab PolD (H451A mutation)	Palud et al., 2008[65]	
Pab PCNA	Palud et al., 2008[65]	
Pab RNase HII, Fen1 and Lig1	Meslet-Cladière et al., 2007[53]	
Trizma® Base, BioUltra for molecular biology, ≥99.8%	Sigma	93362
NaCl, ReagentPlus®, ≥99%	Sigma	S9625
T4 Polynucleotide Kinase (10 U/μL)	ThermoFisher Scientific	EK0031
ATP	Jena Bioscience	NU-1010-10G
DTT	Sigma	D0632
$MgCl_2$	Sigma	M1028-100ML
Formamide	Sigma	EC-608
EDTA	Sigma	E4884-500G
NaOH	Sigma	S9888
dNTPs	Jena Bioscience	NU-1005
TRIzol	Invitrogen	15596026
Chloroform	Sigma	C2432
Isopropanol	Sigma	953716
TE 1X	Sigma	93283-100ML
Proteinase K	Invitrogen	25530031
Sarkosyl	Sigma	61743
SDS	Sigma	436143
RNase A	Thermo Scientific	12091039
MMS	Sigma	129925
MMC	Sigma	M4287
4-NQO	Sigma	N8141
H_2O_2	Sigma	95321
SYBR Gold	Invitrogen	S33102
Critical commercial assays		
QIAEX II Gel Extraction kit	Qiagen	20021
QIAquick Nucleotide Removal kit	Qiagen	28306
RQ1 RNase-free DNase kit	Promega	M6101
iScript™ Reverse Transcription Supermix	Bio-Rad	1708841
SsoAdvanced™ Universal SYBR Green Supermix kit	Bio-Rad	1725270
Deposited data		
Tba*ΔpolB*::Pab*polB* (PAB_RS09320) strain	UBO Culture collection	UBOCC-M-3435
Tba*ΔrnhB*::Pab*rnhB* (PAB_RS02765) strain	UBO Culture collection	UBOCC-M-3436

(*Continued on next page*)

Continued

REAGENT or RESOURCE	SOURCE	IDENTIFIER
Tba*ΔpolB*::Pab*polB* Sequencing data	This paper	NCBI SRA: SRR21319269 Bioproject:PRJNA875043 Biosample: SAMN30594391 https://www.ncbi.nlm.nih.gov/bioproject/PRJNA875043
Tba*ΔrnhB*::Pab*rnhB* Sequencing data	This paper	NCBI SRA: SRR21319268 BioProject:PRJNA875043 Biosample: SAMN30594392 https://www.ncbi.nlm.nih.gov/bioproject/PRJNA875043
Experimental models: Organisms/strains		
Thermococcus barophilus MP	UBO Culture collection	UBOCC-M-3107
Tba*Δ517* (TERMP_RS02570)	UBO Culture collection	UBOCC-M-3300
Tba*ΔpolB* (TERMP_RS08040)	UBO Culture collection	UBOCC-M-3302
Tba*ΔrnhB* (TERMP_RS03345)	UBO Culture collection	UBOCC-M-3303
Tba*ΔpolB*::Pab*polB* (PAB_RS09320)	This paper	UBOCC-M-3435
Tba*ΔrnhB*::Pab*rnhB* (PAB_RS02765)	This paper	UBOCC-M-3436
Oligonucleotides		
Oligonucleotides used for *in vitro* study, see Table S3	Eurogentec	
Primers used for genetic construction, see Table S4	Eurogentec	
Primers used for qPCR, see Table S5	Eurogentec	
Recombinant DNA		
Plasmid: pUPH vector	Birien et al., 2018[32]	
Software and algorithms		
ImageQuant TL 8.1	GE Healthcare	
GraphPad Prism 9.1.0	GraphPad Software	

RESOURCE AVAILABILITY

Lead contact

Further information and requests for resources and reagents should be directed to and will be fulfilled by the lead contact, Ghislaine Henneke (ghislaine.henneke@ifremer.fr).

Material availability

Thermococcus barophilus mutant strains generated in this study have been deposited to UBO Culture Collection (UBOCC-M-3435 and UBOCC-M-3436).

This study did not generate new unique reagents.

Data and code availability

- Whole genome sequencing data (Novogene) of mutant strains have been deposited in the NCBI Sequence Read Archive (SRA) repository and accession numbers are listed in the key resources table. They are publicly available.
- This paper does not report original code.
- Any additional information required to reanalyze the data reported in this paper is available from the lead contact upon request.

EXPERIMENTAL MODEL AND STUDY PARTICIPANT DETAILS

The strains used in this study are described in Table S1. The mutant strains were obtained as in.[32] Briefly, primers used to complement genes of interest are described in Table S4. The inserts obtained were cloned in pUPH plasmid.[32] The resulting plasmids were produced in *E. coli* DH5α cells, followed by extraction and Tba cell transformations according to.[32] The mutant colonies were first selected on plates containing Thermococcales Rich Medium (TRM)[66] supplemented with 2.5 μg/mL of simvastatin (Sigma) and then 100 μM of 6-Methylpurine (Sigma). After PCR selection on Tba clones, the sequences of mutant plasmids and strains were confirmed by Illumina PE150 sequencing (Novogene).

Growth curves were monitored in TRM[66] or Thermococcales Amino Acid (TAA) medium[67] supplemented with sulfur. Cell densities were determined by direct cell counting using a Thoma cell (0.02 mm depth) under a phase contrast Olympus model BH-2 microscope.

For RNA isolation, qRT-PCR analysis and drop dilution assays, TbaWT, TbaΔ*TERMP_00517*, TbaΔ*polB*, TbaΔ*rnhB*, TbaΔ*polB*::Pab*polB*, and TbaΔ*rnhB*::Pab*rnhB* strains were grown in TRM medium supplemented with sulfur at 85°C for 6 hours (log phase).

For the detection of ribonucleotides in genomic DNA experiments, TbaWT, TbaΔ*TERMP_00517*, TbaΔ*polB*, TbaΔ*polB*::Pab*polB*, TbaΔ*rnhB* and TbaΔ*rnhB*::Pab*rnhB* strains were grown in a gas-lift bioreactor under anaerobic conditions at 85°C, pH 6.8 in SME medium.[68–70]

METHOD DETAILS

Enzymes production and purification

The enzymes from *Pyrococcus abyssi* used in this study were cloned, overexpressed and purified as previously described in the following articles: exonuclease deficient versions of PolB (D215A mutation)[64] and PolD (H451A mutation),[65] PCNA,[71] RNase HII, Fen1 and Lig1.[53] Briefly, PolB (D215A mutation) and PolD large subunit genes were inserted in pET28 vector (Novagen), PolD small subunit (H451 mutation) gene was inserted in pARHS vector, PCNA gene was inserted in pET26b(+) vector, RNase HII, Fen1 and Lig1 genes were inserted in pQE-80L vector (Qiagen). The plasmids were introduced in *E. coli* Rosetta 2 (DE3) cells for PolB, in *E. coli* HMS174 (DE3) cells for PolD and PCNA or *E. coli* BL21 (DE3)-CodonPlus-RIL (Stratagene) cells for RNase HII, Fen1 and Lig1. After transformation, cells were grown to an OD_{600} of 0.6 and the protein expression was induced by addition of 1 mM IPTG for PolB, PolD and PCNA or 0.5 mM IPTG for RNase HII, Fen1 and Lig1. Cells were harvested by centrifugation. Cell pellets were resuspended and lysed by sonication on ice before heat shock treatment to remove *E. coli* proteins. After centrifugation, PolB or PolD proteins were purified using a nickel affinity resin (HisTrap HP 5 mL column, GE Healthcare) (linear gradient with increasing imidazole concentration up to 500 mM), a HiTrap Heparin column (HiTrap Heparin HP 5 mL column)(linear gradient with increasing NaCl concentration up to 1 M) and a Superdex^{TM} 200 10/300 GL gel filtration column (GE Healthcare). PCNA proteins were purified successively using an anion-exchange column (HiPrep Q HP 16/10 20 mL column, GE Healthcare)(linear gradient with increasing NaCl concentration up to 1 M) and a hydroxyapatite column (CHT type II 5 mL column, Biorad)(linear gradient with increasing potassium phosphate concentration up to 250 mM). RNase HII, Fen1 and Lig1 proteins were purified using a nickel affinity resin (HisTrap HP 5 mL column, GE Healthcare)(linear gradient with increasing imidazole concentration up to 500 mM) and a Superdex^{TM} 200 10/300 GL gel filtration column (GE Healthcare). Because removal of the Cy5 label at the 3'-end of DNA templates may occur by 3'-5' exonuclease activity of DNA Pols as observed recently,[72] which would have hampered the detection of 3'Cy5 labelled products, reactions are performed with exonuclease-deficient DNA polymerases, thus preventing any disturbance in RER reconstitution.

Oligonucleotides

Oligonucleotides used in this study (Table S3) were purchased from Eurogentec and purified by RP-HPLC with the exception of the 87 bp oligonucleotides, which were purified by PAGE. Oligonucleotides were labelled with FAM or Cy5 fluorophores for detection. Annealing of two or three complementary oligonucleotides was performed in 10 mM Tris-HCl (pH 8) and 50 mM NaCl at a final concentration of 500 nM. The mixture was heated to 95°C for 5 min and slowly cooled to room temperature. For Lig1 assays and Fen1 nuclease activities the oligonucleotide substrates were phosphorylated before annealing. 300 pmol of oligonucleotides were incubated with T4 Polynucleotide Kinase (Thermofisher), in 1X reaction buffer A (Thermofisher) and 1 mM ATP. The mixture was incubated at 37°C for 30 min, heated at 65°C for 20 min. The resulting annealed substrates were gel-purified from excess single-stranded oligonucleotides by the QIAEX II Gel Extraction kit (Qiagen) according to the manufacturer's protocol.

RNase HII, PolB, PolD, Fen1 and Lig1 activity assays

Activity assays were carried out in reaction mixture (20 µL) containing 50 nM of fluorescently labelled oligonucleotide substrate (Table S3), 50 mM Tris-HCl (pH 8), 1 mM DTT, 50 mM NaCl and 5 mM $MgCl_2$ with either 0.05 nM, 0.2 nM, 0.5 nM, 5 nM, 20 nM, 50 nM, 200 nM or 500 nM RNase HII, 12.5 nM, 25 nM, 50 nM, 100 nM, 200 nM, or 250 nM PolB, 50 nM, 100 nM, 200 nM, 400 nM, 800 nM, or 1000 nM PolD, 0.3 µM, 0.75 µM, 1.5 µM, 3 µM or 6 µM Fen1 or 0.3 µM Lig1 (substrates and additional components are mentioned in the figure legends). Fen1 assay were performed with or without the addition of 0.3 µM PCNA or 0.5 µM RNase HII and PolB, PolD and Lig1 assay were performed with or without the addition of 0.3 µM PCNA. RNase HII, Fen1 and Lig1 activity assays were performed at 60°C for 30 min. PolB and PolD strand-displacement activity assays were performed at 60°C for 1 hour. Reactions were stopped on ice by adding one volume of a stop solution containing 86 % formamide, 10 mM EDTA (pH 8), 10 mM NaOH and 1 µM of "oligonucleotide competitor" (the exact complement of the template strand under study) followed by denaturation at 95°C for 3 min.

In vitro RER reconstitution

RER assays were carried out in reaction mixture (30 µL) containing 50 nM of fluorescently dual-labelled oligonucleotide substrate, 50 mM Tris-HCl (pH 8), 1 mM DTT, 50 mM NaCl, 5 mM $MgCl_2$, 1 mM ATP, and all four dNTPs at physiological concentrations (95 µM dATP, 103 µM dGTP, 200 µM dTTP and 33 µM dCTP) as determined previously in *P. abyssi*.[2] Each enzyme activity has been individually studied on proper substrate to determine optimal concentration required for *in vitro* RER reconstitution as mentioned below. Particularly, PolB and PolD concentrations were chosen in order to obtain maximal elongation and strand displacement of the downstream strand. This was a prerequisite to further

evaluate the removal of the resulting full-length ligation products (87-nt in length) by RNase HII treatment. Shorter products were not suitable for such an analysis. The mixtures were incubated at 60°C for 15 min with 500 nM of RNase HII. Then 300 nM of PCNA were added, followed by a further incubation at 60°C for 8 min. Finally, 250 nM of PolB and/or 1 μM of PolD, 300 nM of Fen1 and 300 nM of Lig1 were supplemented to the reaction mixtures, followed by incubation at 60°C for 1 hour. Reactions were stopped on ice. The reaction products were purified using the QIAquick Nucleotide Removal kit (Qiagen) according to the manufacturer's protocol and eluted in 20 μL H_2O. To confirm rNMP removal by RER, half of the reaction mixture (10 μL) was incubated at 55°C for 1 hour in 50 mM Tris-HCl (pH 8) and 5 mM $MgCl_2$ with 500 nM PabRNase HII, whereas the other half of the reaction mixture (10 μL) was without PabRNase HII. Reactions were quenched on ice by adding one volume of a stop solution containing 86 % formamide, 10 mM EDTA (pH 8), 10 mM NaOH and 1 μM of "oligonucleotide competitor" (the exact complement of the template strand under study), followed by denaturation at 95°C for 5 min.

RNA isolation and qRT-PCR analysis

RT-qPCR analysis were performed to assess the level of genes expression in the mutant strains. TbaWT, the parent strain TbaΔ*TERMP_00517*, TbaΔ*polB*, TbaΔ*rnhB* and their respective heterologous complementations TbaΔ*polB*::Pab*polB*, and TbaΔ*rnhB*::Pab*rnhB* strains were grown in TRM medium supplemented with sulfur at 85°C for 6 hours (log phase). Cells were harvested by centrifugation for 6 min, 8000 g at 4°C and suspended in 1 mL Trizol (Invitrogen). 200 μL of pure chloroform (Sigma) were added and samples were gently mixed 10 s and left at room temperature for 3 min. The aqueous phases were collected by centrifugation for 15 min, 13000 g at 4°C. The RNA precipitation was performed by adding 500 μL of isopropanol (Sigma) and incubating at room temperature for 5 min. Cell pellets obtained after centrifugation for 15 min, 13000 g at 4°C were washed two times with ethanol 70 % and air-dried. DNase treatment was done according to manufacturer's protocol (RQ1 RNase-free DNase Kit, Promega). Extracted RNA were quantified by Nanodrop 2000 (ThermoFisher) and 500 ng of RNA were used in Reverse Transcription reaction performed according to the manufacturer's protocol (iScriptTM Reverse Transcription Supermix for RT-qPCR Kit, Bio-Rad). The obtained cDNAs were used in qPCR reaction achieved according to the manufacturer's protocol (SsoAdvancedTM Universal SYBR® Green Supermix Kit, Bio-Rad) with the following incubation program: 30 s at 95°C, 40 cycles amplification (15 s at 95°C, 30 s at 60°C), Melting curve (65°C to 95°C with 0.5°C increments, 5 s by step). Primers used for qPCR reaction are described in Table S5.

Detection of ribonucleotides in genomic DNA

TbaWT, the parental strain TbaΔ*TERMP_00517*, TbaΔ*polB*, TbaΔ*polB*::Pab*polB*, TbaΔ*rnhB* and TbaΔ*rnhB*::Pab*rnhB* strains (Table S1) were grown in a gas-lift bioreactor under anaerobic conditions at 85°C, pH 6.8 in SME medium.[68–70] Logarithmically growing cells were harvested by centrifugation for 1 hour, 8000 g at 4°C. The detection of ribonucleotides in genomic DNA was done by alkaline treatment as described in[2] with some modifications. Cell pellets (~1 g) were suspended in 3.2 mL TE 1X (Sigma). Cell lysis was performed by adding 200 μL Proteinase K (20 mg/mL), 400 μL Sarkosyl (10 %) (Sigma) and 400 μL SDS (10 %) (Sigma) followed by incubation at 37°C for 1.5 hours. Isolation of total DNA was achieved according to[2] except RNase A treatment which was done in TE 1X (Sigma), NaCl (0.5 M). RNase A in the presence of 0.5 M NaCl allows the selective degradation of single-stranded RNA without degrading embedded ribonucleotides in genomic DNA.[22,73,74] Ribonucleotide detection was performed by incubation of genomic DNA for 2h at 55°C with either 0.3 M NaCl or NaOH as described in.[2] Then, samples were ethanol precipitated before separation on 1x TBE agarose gel (1%) electrophoresis under neutral conditions [5% glycerol, 1.7 mM Tris–HCl (pH 8), 0.17 mM Na_2EDTA] or after denaturation with 90% formamide and 20 mM EDTA.

Drop dilution assays

Drop dilution assays protocol was adapted from.[75,76] TbaWT, the parental strain TbaΔ*TERMP_00517*, TbaΔ*polB*, TbaΔ*rnhB* and their respective heterologous complementation TbaΔ*polB*::Pab*polB* and TbaΔ*rnhB*::Pab*rnhB* strains were grown in TRM medium at 85°C for 6 hours (log phase). 1 mL of cells culture were harvested by centrifugation for 6 min, 8000 g at 4°C and suspended in 100 μL of TRM supplemented with 0.015 %, 0.1 % or 0.2 % Methyl Methane-Sulfonate (MMS, Sigma), 20, 30 or 100 μg/mL MitoMycin C (MMC, Sigma), 5 or 10 μM 4-NitroQuinoline N-Oxide (4-NQO, Sigma) or 30 or 400 μM hydrogen peroxide (H_2O_2, Sigma) and incubated at room temperature for 4 hours. Cells are then harvested by centrifugation for 6 min, 8000 g at 4°C and suspended in TRM (10 μL). Cells were diluted to 1.10^6, 1.10^5, 1.10^4, 1.10^3 and 1.10^2 and 2 μL of each dilution were spotted on solid TRM medium (1 % phytagel, TRM, 0.5 g/L colloidal sulfur). After 5 days of incubation at 85°C, the colonies on plates were transferred to polyvinylidene fluoride membranes and stained with Coomassie Blue.

QUANTIFICATION AND STATISTICAL ANALYSIS

Visualisation and quantification of fluorescently labelled products

Reaction products were resolved on 12% denaturing polyacrylamide 8 M urea gels. Labelled oligonucleotides were detected with Typhoon FLA 9500 (GE Healthcare) and quantified with ImageQuant TL 8.1 software (GE Healthcare) as published previously.[2] The different products (obtained by RNase HII or Fen1 cleavage, extension by Pol or ligation by Lig1) were quantified as the intensity of the corresponding band as a percentage of total lane intensity. In RER reconstitution, the starting substrate consists of double-stranded DNA containing a matched rA/dT or mismatched rA/dC base pair. The top oligonucleotide strand (87-nt) that harbors the rAMP is dual-labelled with a Cy5 (green label) and a 6-FAM dye (red label) at the 3' and 5' ends, respectively. Dual-labelling allows the detection of different reaction products in each panel. In the Cy5 panel, 87-nt, uncleaved dual-labelled rAMP-containing oligonucleotide substrates, 30-nt RNase HII incised products, 29-nt Fen1 cleavage products, 31-nt ligation failure products and the resulting repaired dual-labelled 87-nt ligation products are detectable. In the Fam panel,

87-nt uncleaved dual-labelled rAMP-containing oligonucleotide substrates, 57-nt RNase HII incised products, 87-nt single-stranded extension products, and the resulting repaired dual-labelled 87-nt ligation products are detectable. Because of the presence of the two dyes at the 3′ and 5′ ends, 87-nt dual-labeled ligation products migrate at a position higher than 5′Fam labeled 87-nt extension products which contain only one dye. Dual-labelled ligation products obtained in RER reconstitution (Figures 2, S2, and S3) were quantified from the fluorescence visualization of bands in Cy5 panel gels. The mean and standard deviation of the reaction products quantification are represented as histogram in the figures. The number of independent experiments is described in the figure legends. p-values were determined by unpaired t-test and are reported: ***p-value < 0.0001, *p-value < 0.05 and non-significant (p-value > 0.05) (ns).

RNA isolation and qRT-PCR analysis

The relative expressions were calculated according to the $2^{-\Delta\Delta Ct}$ method using 30S as endogenous control.[77] The number of independent experiments is described in the figure legends.

Detection of ribonucleotides in genomic DNA

Products were separated on 1 x TBE neutral agarose gel. Gels were stained with SYBR Gold® (Invitrogen). Densitometry traces were obtained with ImageQuant TL 8.1 software (GE Healthcare) and plotted as follows: each lane profile was extracted from the gel image and the background subtracted.